

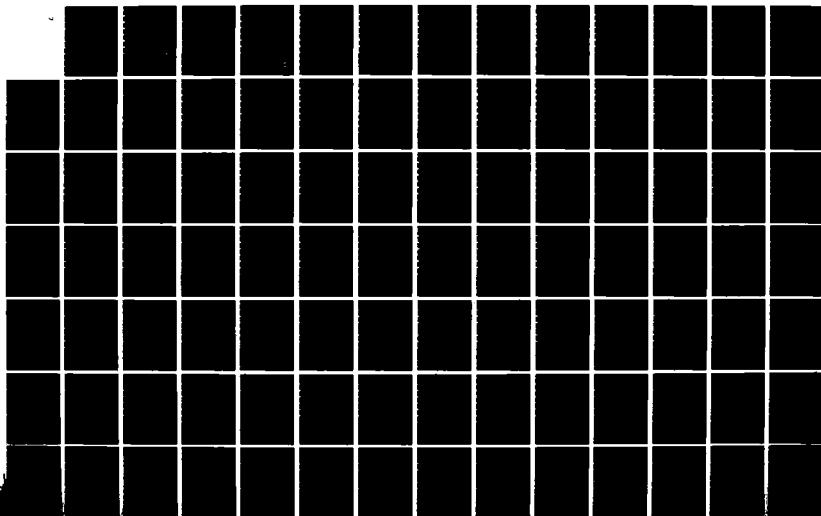
AD-A141 062

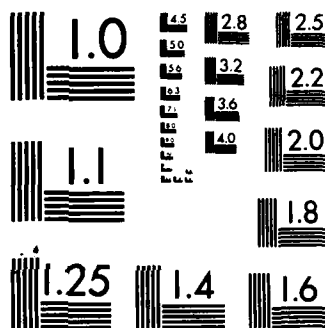
AN ANALYTICAL STUDY OF A LOCALLY COOLED HIGH REYNOLDS
NUMBER SIMULATION TECHNIQUE(U) AIR FORCE INST OF TECH
WRIGHT-PATTERSON AFB OH SCHOOL OF ENGI... N S BORKOWSKI
MAR 84 AFIT/GA/AA/84M-1 F/G 20/4

1/2

UNCLASSIFIED

NL





MICROCOPY RESOLUTION TEST CHART
NATIONAL BUREAU OF STANDARDS-1963-A

①

AD-A141 062

DTIC FILE COPY

AN ANALYTICAL STUDY OF A
LOCALLY COOLED HIGH REYNOLDS NUMBER
SIMULATION TECHNIQUE

THESIS

Presented to the Faculty of the School of Engineering
of the Air Force Institute of Technology

Air Training Command
in Partial Fulfillment of the
Requirements for the Degree of
Master of Science

by

Mark S. Borkowski, B.S., B.S.A.E.
First Lieutenant USAF
Graduate Astronautical Engineering
March, 1984

DTIC
ELECTE
S MAY 15 1984
A

AFIT/GA/AA/84M-1

AN ANALYTICAL STUDY OF A
LOCALLY COOLED HIGH REYNOLDS NUMBER
SIMULATION TECHNIQUE

THESIS

AFIT/GA/AA/84M-1

Mark S. Borkowski
1st Lt. USAF

Approved for Public Release; distribution unlimited

UNCLASSIFIED

SECURITY CLASSIFICATION OF THIS PAGE

REPORT DOCUMENTATION PAGE

1a. REPORT SECURITY CLASSIFICATION UNCLASSIFIED			1b. RESTRICTIVE MARKINGS	
2a. SECURITY CLASSIFICATION AUTHORITY			3. DISTRIBUTION/AVAILABILITY OF REPORT Approved for public release; distribution unlimited	
2b. DECLASSIFICATION/DOWNGRADING SCHEDULE				
4. PERFORMING ORGANIZATION REPORT NUMBER(S) AFIT/GA/AA/84M-1			5. MONITORING ORGANIZATION REPORT NUMBER(S)	
6a. NAME OF PERFORMING ORGANIZATION AFIT		6b. OFFICE SYMBOL (If applicable) ENY		7a. NAME OF MONITORING ORGANIZATION
6c. ADDRESS (City, State and ZIP Code) Wright-Patterson AFB, OH 45433			7b. ADDRESS (City, State and ZIP Code)	
8a. NAME OF FUNDING/SPONSORING ORGANIZATION		8b. OFFICE SYMBOL (If applicable)		9. PROCUREMENT INSTRUMENT IDENTIFICATION NUMBER
8c. ADDRESS (City, State and ZIP Code)			10. SOURCE OF FUNDING NOS.	
			PROGRAM ELEMENT NO.	PROJECT NO.
			TASK NO.	WORK UNIT NO.
11. TITLE (Include Security Classification) An Analytical Study of Locally Cooled				
12. PERSONAL AUTHOR(S) High Reynolds Number Simulation Technique (Unclassified) Borkowski, Mark S.				
13a. TYPE OF REPORT MS Thesis		13b. TIME COVERED FROM _____ TO _____		14. DATE OF REPORT (Yr., Mo., Day) 1984 March
				15. PAGE COUNT 94
16. SUPPLEMENTARY NOTATION Approved for public release LAW AFB 190-17. E. E. WOLAVER 7 May 84 Data for Research and Professional Development Wright-Patterson AFB OH 45433				
17. COSATI CODES			18. SUBJECT TERMS (Continue on reverse if necessary; use block number)	
FIELD	GROUP	SUB. GR.	Boundary Layer Theory	
20	04		Wind Tunnel Testing	
			Reynolds Number Simulation	
19. ABSTRACT (Continue on reverse if necessary and identify by block number) An analytical study of a technique for achieving high Reynolds number similarity in a wind tunnel was conducted. The technique under consideration required that the momentum boundary layer be immersed in a layer of cryogenically cooled gas so that boundary layer development would be determined by the low temperature fluid properties. The experimental technique was shown to be feasible, with effective Reynolds number increased by as much as a factor of seven or eight, provided that sufficiently high mass rates of flow of cool gas could be provided				
20. DISTRIBUTION/AVAILABILITY OF ABSTRACT UNCLASSIFIED/UNLIMITED <input checked="" type="checkbox"/> SAME AS RPT. <input type="checkbox"/> DTIC USERS <input type="checkbox"/>			21. ABSTRACT SECURITY CLASSIFICATION UNCLASSIFIED	
22a. NAME OF RESPONSIBLE INDIVIDUAL Wesley R. Cox, Capt, USAF			22b. TELEPHONE NUMBER (Include Area Code) (513) 255-3708	22c. OFFICE SYMBOL AFIT/ENY

DD FORM 1473, 83 APR

EDITION OF 1 JAN 73 IS OBSOLETE.

84 05 14 111

UNCLASSIFIED
SECURITY CLASSIFICATION OF THIS PAGEDTIC
ELECTE

MAY 15 1984

Preface

I shall always be grateful to the people who assisted me in the completion of this thesis. The members of my committee have been very good to me: I owe a great deal to Dr. (1st Lt) Dale Carlson, Professor James Hitchcock, and Professor Harold Larsen. I learned from each of them, and I appreciated their efforts in helping me over the rough spots.

I would especially like to thank my advisor, Dr. (Capt) Wesley Cox, for his encouragement and support over the course of this study. His easy going, but firm guidance has been very much appreciated.

My friends have been instrumental in keeping my spirits up during my time at AFIT. I would particularly like to thank the members of my first AFIT class, UGA-83M, for all of the support they have always given me.

1Lt Caralee A. Capone has been a constant friend and confidant over the past 2½ years; I will always be grateful to her for that.

Finally, I would like to thank Leslie and Natalie for having given me a sense of perspective at very critical times.

Mark Borkowski



A1

Contents

Preface	ii
List of Figures	iv
List of Tables	v
Notation	vi
Abstract	ix
I. Introduction	1
Background	2
Purpose	6
II. Theory	8
Continuity Equation	9
Momentum Equation	9
Energy Equation	11
III. Reynolds Similarity and Wind Tunnel Testing	13
IV. Development of a High Reynolds Number Simulation Technique .	17
Momentum Mixing	19
Thermal Mixing	21
Condensation/Icing	25
Other Considerations	28
V. High Reynolds Number Simulation: The Flat Plate	31
VI. A Proposed Experimental Design	41
VII. Conclusions and Recommendations	48
Bibliography	50
Appendix A: The Governing Equations for Viscous Fluid Flow	52
Appendix B: The Thermal Mixing Region	60

Appendix C: Condensation and Icing	69
Appendix D: Property Values and Sample Calculations	76
Appendix E: The Parameter L	82
Vita	85

List of Figures

Figure

1.	Development of the Momentum Boundary Layer Within a Layer of Cool Fluid	7
2.	Velocity Profiles for (a) Velocity Discontinuity and (b) Momentum Mixing Region	18
3.	The Thermal Mixing Region	18
4.	Boundary Layer Development and Cool Fluid Layer Over a Flat Plate	32
5.	Detail of Experimental Design	42
B.1.	Development of the Thermal Mixing Region . . .	61
E.1.	Functional Dependence of L on Temperature for (a) Laminar Flow and (b) Turbulent Flow with $l = 2$ ft	84

List of Tables

Table

1.	Distance Fallen by a Spherical Particle of Diameter = 0.01 ft	27
C.1.	Comparison of Equations C.3 and C.4 with Measured Data	72
C.2.	Results of the Numerical Integration of Equation C.7 ($\Delta t = 0.1$ sec)	75
C.3.	Results of the Numerical Integration of Equation C.7 ($\Delta t = 0.01$ sec)	75

Notation

A	Frontal Area
a	Thickness
a	Speed of Sound
b	Half-Width of Momentum Mixing Region
b_t	Half-Width of Thermal Mixing Region
Bi	Biot Number
c_p	Constant Pressure Specific Heat
C_D	Coefficient of Drag
c_f	Coefficient of Friction
E	Energy per Unit Mass
e	Internal Energy per Unit Mass
f	Body Force per Unit Mass
g	Acceleration of Gravity
Gr	Grashof Number
h	Convective Heat Transfer Coefficient
h	Enthalpy per Unit Mass
h	Height of Layer of Cool Fluid
$\bar{\mathbf{I}}$	Identity Tensor
$\hat{\mathbf{i}}, \hat{\mathbf{j}}, \hat{\mathbf{k}}$	Cartesian Unit Vectors
k	Thermal Conductivity
L	L-parameter, the ratio $h/\sqrt{\mathcal{L}}$
ℓ	Length
M	Mach Number
M	Molecular Weight
\dot{m}	Mass Rate of Flow

\hat{n}	Normal Unit Vector
Nu	Nusselt Number
p	Pressure
q	Dynamic Pressure
\bar{q}	Heat Flux Vector
R	Degrees Rankine
R	Gas Constant
\tilde{R}	Universal Gas Constant
r	Radius
Re	Reynolds Number
S	Surface Area
T	Temperature
t	Time
u	Velocity Component in Streamwise Direction
v	Velocity Component Normal to Streamwise Direction
V	Velocity
Vol	Volume
\bar{v}	Velocity Vector
w	Width
x_i	Arc Length in i^{th} Coordinate Direction

Greek Symbols

α	Thermal Diffusivity
β	Empirical Constant
γ	Ratio of Specific Heats
δ	Momentum Boundary Layer Thickness

$\partial\Omega$	Surface which Bounds the Region Ω
ζ	$\log_{10} C_D$
η	Similarity Variable
θ	Non-Dimensional Temperature Difference
λ	Second Coefficient of Viscosity
μ	First Coefficient of Viscosity
ν	Coefficient of Kinematic Viscosity
ξ	$\log_{10} Re$
ρ	Density
$\vec{\sigma}$	Stress Vector
$\overline{\overline{\sigma}}$	Stress Tensor
τ	Shear Stress
$\overline{\overline{\tau}}$	Shear Stress Tensor
Φ	Viscous Dissipation
Ω	Control Volume

Subscripts

c	Cooled
ℓ	Laminar
m	Momentum
n	Normal Component
p	Spherical Particle
s	Static
t	Thermal
t	Turbulent
w	Wall Conditions
∞	Free Stream

Abstract

An analytical study of a technique for achieving high Reynolds number similarity in a wind tunnel was conducted. The technique under consideration required that the momentum boundary layer be immersed in a layer of cryogenically cooled gas so that boundary layer development would be determined by the low temperature fluid properties. The experimental technique was shown to be theoretically feasible, with effective Reynolds number increased by as much as a factor of seven or eight, provided that sufficiently high mass rates of flow of cool gas could be provided.

AN ANALYTICAL STUDY OF A
LOCALLY COOLED HIGH REYNOLDS NUMBER
SIMULATION TECHNIQUE

I. Introduction

Aerodynamic structures are often tested in wind tunnels to predict their free flight performance. The aerodynamic forces on a structure strongly depend on the Reynolds number, so it is important that the free flight value of this parameter be matched as closely as possible by tunnel test conditions. Due to the limited scale size of models that are used in wind tunnel testing, however, this requirement cannot always be properly met. Many free flight conditions of interest have not been adequately simulated using current techniques.

There is a desire to develop new procedures which might remove some of the existing constraints on wind tunnel Reynolds numbers. The study of this paper is concerned specifically with a proposal to simulate high Reynolds number flight conditions by locally immersing the model being tested in an envelope of cold fluid. Because the Reynolds number increases significantly as temperature decreases, it is hoped that such a technique could increase the effective wind tunnel Reynolds number by as much as an order of magnitude.

Background

Wind tunnel testing is based on the premise that the fluid flow around a scale model of a structure will be similar in some sense to a fluid flow around the full scale structure itself. In the case where the fluid flow is inviscid and incompressible, this premise would allow the results of a tunnel test to be extended to an arbitrary situation as a function of the scale of the model and of the free stream velocity of the fluid.

Unfortunately, real fluids are neither inviscid nor incompressible. This is a significant complication, since compressibility and viscosity are dependent on the particular conditions for which they are being measured. Consequently, it is not immediately apparent how results based on the effects of viscosity and compressibility in a wind tunnel can be used to make predictions about the behavior of a structure in the general case.

In order to gain insight into the question of how wind tunnel test results can be extended to other situations, it is convenient to non-dimensionalize the equations which describe the behavior of real fluids. When this is done, two parameters appear to be of major significance when the fluid flows around two geometrically similar structures are to be compared.

The first of these parameters is the Reynolds number. Denoted by Re , and determined from the relationship $Re =$

$\frac{\rho V \ell}{\mu}$, the Reynolds number is a measure of the ratio between the inertia force of the flow and the force which results from viscous effects.

The second parameter is the Mach number, which is determined from the relationship $M = \frac{V}{a}$. Commonly known as the ratio of local velocity to local speed of sound, the Mach number is a measure of the way in which a disturbance in the flow field (an airfoil, for instance) may effect the fluid flow upstream from the disturbance.

When the aerodynamic forces on a structure are non-dimensionalized with respect to dynamic pressure ($q = \frac{1}{2}\rho V^2$) and to some characteristic area, theoretical and empirical results suggest that these non-dimensionalized forces are functions primarily of the Reynolds and Mach numbers. Therefore, the aerodynamic forces on a structure can be used to predict the aerodynamic forces on a geometrically similar structure if the Mach and Reynolds numbers for the two flow situations are the same.

In principle, the behavior of an aerodynamic structure in free flight can be predicted from wind tunnel tests on a scale model if the tunnel Mach number and Reynolds number can be set equal to the free stream values of those parameters.

This principle cannot often be applied in practice. Wind tunnels are limited in the range of Mach and Reynolds numbers over which tests can be conducted, and it is rarely possible to simulate the free stream values of these two

parameters simultaneously.

There are some flow situations of practical interest where the dependence of aerodynamic forces on the Mach number is negligible (when $M = 0.3-0.5$ or less, see ref 1). In these cases, wind tunnel test results can be used to give good predictions of free flight behavior if Reynolds number similarity can be obtained in the wind tunnel.

Even in this case where Mach similarity is insignificant there are substantial constraints on wind tunnel testing.

In an attempt to simulate high Reynolds number conditions, the wind tunnel experimentalist may try to adjust the free stream tunnel velocity (V), the characteristic length of the model (ℓ), or the kinematic viscosity of the fluid ($\nu \equiv \mu/\rho$).

The tunnel velocity is limited by the ability of the tunnel to accelerate the flow. There is an upper limit to the velocity that can be achieved in the test section of a wind tunnel. Furthermore, high tunnel velocities result in high test Mach numbers, so that compressibility effects have a significant impact on the test results in spite of the fact that compressibility may not be important in the free flight situation to be simulated.

The characteristic length of the model is obviously limited by the size of the tunnel test section. Although large tunnels could be built, tremendous amounts of power would be required to drive such a tunnel.

The kinematic viscosity has a rather strong dependence on pressure and temperature. Kinematic viscosity decreases with increased pressure or decreased temperature, so high pressures or low temperatures can be used to obtain high Reynolds number simulation in a wind tunnel.

The National Transonic Facility (NTF), currently being constructed for NASA at Langley, Virginia, will combine increased pressure and cryogenic temperatures in order to simulate high Reynolds number flow (ref 2).

There are other techniques which can be used to simulate high Reynolds number flow. Since such flows are generally characterized by turbulent boundary layers, turbulence can be induced over the structure to be tested (through use of roughness or "trip wires," for example; see ref 3), thereby simulating high Reynolds number flow in an otherwise low Reynolds number situation. Another technique involves testing several different size models with similar geometries and attempting to extrapolate the results from these tests to appropriately sized structures.

Each of the techniques described above has drawbacks, typically with respect to added expense of the test procedure, added complexity of the scale model to be tested, or theoretical difficulty in extending test results to the free flight situation of interest. Therefore, a relatively simple, low cost means of providing high Reynolds number simulation is clearly desirable.

One possibility for such a technique has been sug-

gested by W. Luchuk of the Air Force Arnold Engineering Development Center (ref 4). Mr. Luchuk has proposed that high Reynolds number simulation could be obtained locally by injecting a cryogenic fluid to envelop the momentum boundary layer.

Purpose

The purpose of this study is to analyze the potential of a high Reynolds number simulation technique which accomplishes boundary layer cooling through the introduction of a cool gas over the structure to be tested.

In this paper, the major considerations that must go into the development of a locally high Reynolds number simulation technique are outlined and discussed. These considerations are then applied to establish the important physical parameters for such a technique and to make conclusions regarding the feasibility of the technique.

The flow situation of interest is illustrated in fig 1. In particular, the case for flow over a flat plate will be studied in detail.

The results of the analysis described above are discussed at the end of this paper, and recommendations for additional study are also included there.

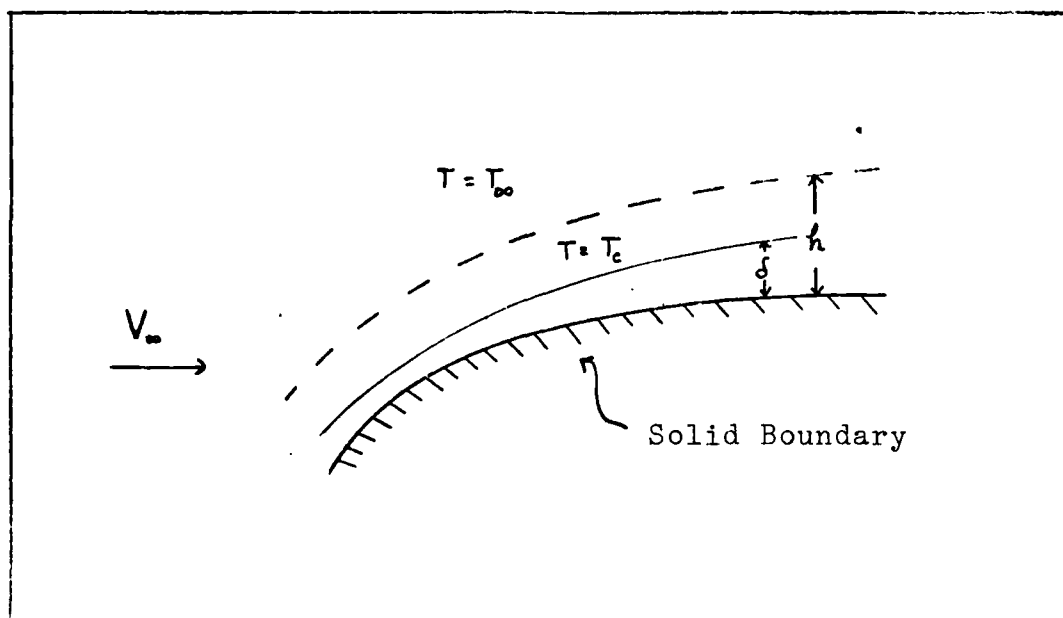


Figure 1. Development of the Momentum Boundary Layer
Within a Layer of Cool Fluid

II. Theory

The mathematical model which is used to describe the behavior of a fluid is typically developed from an Eulerian, or "Control Volume," point of view. From this point of view, the laws of physics which require conservation of mass, momentum, and energy of a fixed mass system are adapted to predict behavior in and around a fixed region in space.

The Eulerian analogs to the fixed mass concepts of conservation of mass, Newton's Second Law, and conservation of energy are, respectively, the Continuity Equation, the Momentum Equation, and the Energy Equation.

These equations are presented below in two forms. In the first case, they are presented in tensorial form so that they may be applied to any flow situation describable in terms of an orthogonal coordinate system. The principles which are applied to the case of a flat plate can then be extended to apply to arbitrary shapes when an appropriate coordinate system has been defined.

In the second case, the equations are presented in the well known form for rectangular (Cartesian) coordinate systems.

Appendix A to this report gives a detailed mathematical derivation of the governing equations from a tensor analysis point of view.

The Continuity Equation

The amount of mass contained within a control volume may change with time. This change can be the result of a change in the density of the mass contained within the volume due to an influx of mass to the control volume. This is expressed as

$$\frac{D\rho}{Dt} + \rho(\nabla \cdot \bar{v}) = 0 \quad (1)$$

In terms of Cartesian coordinates, with $\bar{v} = u\hat{i} + v\hat{j} + w\hat{k}$, this is written

$$\frac{\partial \rho}{\partial t} + u \frac{\partial \rho}{\partial x} + v \frac{\partial \rho}{\partial y} + w \frac{\partial \rho}{\partial z} + \rho \left(\frac{\partial u}{\partial x} + \frac{\partial v}{\partial y} + \frac{\partial w}{\partial z} \right) = 0 \quad (2)$$

In the case where density can be assumed to be constant, these equations reduce to

$$(\nabla \cdot \bar{v}) = 0 \quad (3)$$

$$\frac{\partial u}{\partial x} + \frac{\partial v}{\partial y} + \frac{\partial w}{\partial z} = 0 \quad (4)$$

The Momentum Equation

The momentum within a control volume can change with time due to changes in properties in the control volume caused by the transfer of momentum into the control volume

or due to the action of forces on the mass inside the volume.

In the case where the shear stresses acting on the boundary of the control volume are linearly dependent on the rate of deformation of the mass contained within the volume, the momentum equation is given by

$$\rho \frac{D\bar{v}}{Dt} = -\nabla p + \nabla(\lambda \nabla \cdot \bar{v}) + \nabla \cdot \mu (\nabla \bar{v} + \text{grad } \bar{v}) + \rho \bar{f} \quad (5)$$

Equation (5) is really a system of three scalar equations, the Navier-Stokes equations, which are written in Cartesian coordinates as

x-direction:

$$\begin{aligned} \rho \left(\frac{\partial u}{\partial t} + u \frac{\partial u}{\partial x} + v \frac{\partial u}{\partial y} + w \frac{\partial u}{\partial z} \right) &= X - \frac{\partial p}{\partial x} \\ &+ \frac{\partial}{\partial x} \left\{ \mu \left(2 \frac{\partial u}{\partial x} - \frac{2}{3} \left(\frac{\partial u}{\partial x} + \frac{\partial v}{\partial y} + \frac{\partial w}{\partial z} \right) \right) \right\} \\ &+ \frac{\partial}{\partial y} \left\{ \mu \left(\frac{\partial u}{\partial y} + \frac{\partial v}{\partial x} \right) \right\} + \frac{\partial}{\partial z} \left\{ \mu \left(\frac{\partial w}{\partial x} + \frac{\partial u}{\partial z} \right) \right\} \end{aligned}$$

y-direction:

$$\begin{aligned} \rho \left(\frac{\partial v}{\partial t} + u \frac{\partial v}{\partial x} + v \frac{\partial v}{\partial y} + w \frac{\partial v}{\partial z} \right) &= Y - \frac{\partial p}{\partial y} \\ &+ \frac{\partial}{\partial y} \left\{ \mu \left(2 \frac{\partial v}{\partial y} - \frac{2}{3} \left(\frac{\partial u}{\partial x} + \frac{\partial v}{\partial y} + \frac{\partial w}{\partial z} \right) \right) \right\} \\ &+ \frac{\partial}{\partial z} \left\{ \mu \left(\frac{\partial v}{\partial z} + \frac{\partial w}{\partial y} \right) \right\} + \frac{\partial}{\partial x} \left\{ \mu \left(\frac{\partial v}{\partial x} + \frac{\partial u}{\partial y} \right) \right\} \end{aligned} \quad (6)$$

z-direction:

$$\begin{aligned} \rho \left(\frac{\partial w}{\partial t} + u \frac{\partial w}{\partial x} + v \frac{\partial w}{\partial y} + w \frac{\partial w}{\partial z} \right) &= Z - \frac{\partial p}{\partial z} \\ &+ \frac{\partial}{\partial z} \left\{ \mu \left(2 \frac{\partial w}{\partial z} - \frac{2}{3} \left(\frac{\partial u}{\partial x} + \frac{\partial v}{\partial y} + \frac{\partial w}{\partial z} \right) \right) \right\} \\ &+ \frac{\partial}{\partial x} \left\{ \mu \left(\frac{\partial w}{\partial x} + \frac{\partial u}{\partial z} \right) \right\} + \frac{\partial}{\partial y} \left\{ \mu \left(\frac{\partial w}{\partial y} + \frac{\partial v}{\partial z} \right) \right\} \end{aligned}$$

In the case where body forces can be neglected and properties can be assumed constant, these equations become

$$\rho \frac{D\bar{v}}{Dt} = -\nabla p + \mu \nabla^2 \bar{v} \quad (7)$$

x-direction:

$$\rho \left(\frac{\partial u}{\partial t} + u \frac{\partial u}{\partial x} + v \frac{\partial u}{\partial y} + w \frac{\partial u}{\partial z} \right) = -\frac{\partial p}{\partial x} + \mu \left(\frac{\partial^2 u}{\partial x^2} + \frac{\partial^2 u}{\partial y^2} + \frac{\partial^2 u}{\partial z^2} \right)$$

y-direction:

$$\rho \left(\frac{\partial v}{\partial t} + u \frac{\partial v}{\partial x} + v \frac{\partial v}{\partial y} + w \frac{\partial v}{\partial z} \right) = -\frac{\partial p}{\partial y} + \mu \left(\frac{\partial^2 v}{\partial x^2} + \frac{\partial^2 v}{\partial y^2} + \frac{\partial^2 v}{\partial z^2} \right) \quad (8)$$

z-direction:

$$\rho \left(\frac{\partial w}{\partial t} + u \frac{\partial w}{\partial x} + v \frac{\partial w}{\partial y} + w \frac{\partial w}{\partial z} \right) = -\frac{\partial p}{\partial z} + \mu \left(\frac{\partial^2 w}{\partial x^2} + \frac{\partial^2 w}{\partial y^2} + \frac{\partial^2 w}{\partial z^2} \right)$$

The Energy Equation

The energy contained within a fixed region of space may change with time due to the addition of mass or heat to the control volume and due to work done on the control volume. When this statement is expressed mathematically, the resulting equation can be combined with the momentum equation to yield the thermal energy equation

$$\rho \frac{De}{Dt} = -p \nabla \cdot \bar{v} - \nabla \cdot \bar{q} + \phi \quad (9)$$

For a perfect gas, and when viscous dissipation is negligible, equation (9) reduces to the form

$$\rho c_p \frac{DT}{Dt} = \frac{Dp}{Dt} - \nabla \cdot \bar{q} \quad (10)$$

Application of Fourier's Law and the assumption of constant properties gives the familiar form

$$\frac{DT}{Dt} = \alpha \nabla^2 T \quad (11)$$

which is written in terms of Cartesian coordinates as

$$\frac{\partial T}{\partial t} + u \frac{\partial T}{\partial x} + v \frac{\partial T}{\partial y} + w \frac{\partial T}{\partial z} = \alpha \left(\frac{\partial^2 T}{\partial x^2} + \frac{\partial^2 T}{\partial y^2} + \frac{\partial^2 T}{\partial z^2} \right) \quad (12)$$

III. Reynolds Similarity and Wind Tunnel Testing

From the presentation above it is clear that the momentum equation is coupled to the energy equation since the fluid properties are dependent on the thermodynamic state of the fluid. In terms of its effect on wind tunnel testing, it is this coupling which results in the requirement that tunnel values of Re and M should be simultaneously set equal to their free flight values.

In many practical applications it is reasonable to treat the fluid properties as essentially constant. In this case the momentum equation is uncoupled from the energy equation and the velocity profile of the fluid can be obtained from the momentum equation alone. Since aerodynamic forces on a structure are dependent on the velocity profile of the fluid surrounding it, the aerodynamic forces will be independent of the properties of the energy equation and will depend on the properties of the momentum equation alone when fluid properties are constant.

In order to study the properties of the momentum equation it is convenient to express it in non-dimensional terms. To this end, reference values for each of the quantities of interest are defined and non-dimensional expressions for those quantities are defined by referring each to its reference value.

These non-dimensional terms are denoted with a superscript cross (+) and are defined as

$$\begin{aligned} t^+ &= t/(\ell/V_\infty) & p^+ &= (p-p_\infty)/\rho_\infty V_\infty^2 & x_i^+ &= x_i/\ell \\ \bar{v}^+ &= \bar{v}/V_\infty & \lambda^+ &= \lambda/\lambda_\infty & \mu^+ &= \mu/\mu_\infty \\ \rho^+ &= \rho/\rho_\infty & \nabla^+ &= \ell \nabla \end{aligned} \quad (13)$$

Substituting for the dimensional quantities in equation (5), the result is

$$\frac{\rho_\infty V_\infty^2}{\ell} \rho^+ \frac{D\bar{v}^+}{Dt^+} = - \frac{\rho_\infty V_\infty^2}{\ell} \nabla^+ p^+ + \frac{\lambda_\infty V_\infty}{\ell^2} \nabla^+ (\lambda^+ \nabla^+ \cdot \bar{v}^+) + \frac{\mu_\infty V_\infty}{\ell^2} \nabla^+ \cdot (\mu^+ \text{def}^+ \bar{v}^+) \quad (14)$$

where $\text{def}^+ \bar{v}^+ = \nabla^+ \bar{v}^+ + \text{grad}^+ \bar{v}^+$.

Combining terms and simplifying gives the result

$$\rho^+ \frac{D\bar{v}^+}{Dt^+} = - \nabla^+ p^+ + (1/\text{Re}_{\infty, \lambda}) \nabla^+ (\lambda^+ \nabla^+ \cdot \bar{v}^+) + (1/\text{Re}_\infty) \nabla^+ \cdot (\mu^+ \text{def}^+ \bar{v}^+) \quad (15)$$

where $\text{Re}_{\infty, \lambda} = \frac{V_\infty \rho_\infty \ell}{\lambda_\infty}$ and $\text{Re}_\infty = \frac{V_\infty \rho_\infty \ell}{\mu_\infty}$.

The quantity Re is the Reynolds number.

In the case of constant properties, ρ^+ , μ^+ , and λ^+ are all equal to unity, so the non-dimensional momentum equation takes the form

$$\frac{D\bar{v}^+}{Dt^+} = (1/\text{Re}_{\infty, \lambda}) \nabla^+ (\nabla^+ \cdot \bar{v}^+) + (1/\text{Re}_\infty) \nabla^+ \cdot (\text{def}^+ \bar{v}^+) - \nabla^+ p^+ \quad (16)$$

If two flows have the same geometry (so that the

pressure gradient and boundary conditions are the same for both) and if the assumption of constant properties applies equally to the two, they will have the same solution to equation (16) if they have the same value of Reynolds number.

When a fluid in motion encounters a solid surface, the fluid and the surface will exert forces on each other. The magnitude of these forces is related to the development of the boundary layer (the region in which the solid object has a significant effect on the flow field). It is clear from equation (16) that the development of the boundary layer is dependent on the Reynolds number, so the shear forces are dependent on Re as well. In particular, when the shear stress, τ , is non-dimensionalized in terms of a friction coefficient, $c_f = \tau / (\frac{1}{2} \rho_\infty V_\infty^2)$, this coefficient is a function of the Reynolds number (ref 1).

If two flows are geometrically similar and if they have the same Reynolds number, they will have the same value of c_f .

Wind tunnel testing is based on this concept of similarity. A scale model of a structure can be placed in a wind tunnel and values of c_f as a function of Re can be determined. These values of c_f can then be applied to predict the behavior of the full scale structure.

Unfortunately, the concept of Reynolds similarity breaks down for high values of Re and simulation of high Reynolds numbers typically is not achieved. Chapter I of this report has detailed some of the reasons for the

failure of this similarity concept and has suggested the desirability of designing techniques to permit high Reynolds number simulation.

To obtain high Reynolds numbers on sub-scale models, attention has been focused on the possibility of varying the quantity ν ($\nu = \mu/\rho$) which appears in the definition of Re. Since the value of ν decreases with a decrease in temperature for a gas, cooling techniques can be used to provide high Reynolds number simulation.

The remainder of this paper is concerned with one possible technique for the use of cooling.

If a cool gas can be introduced into the tunnel free stream so that the structure being tested is enveloped entirely by the cool fluid, the Reynolds number in the vicinity of the structure will be significantly greater than the Reynolds number based on properties of the tunnel free stream fluid.

Results to be presented elsewhere in this paper will suggest that the use of sufficiently cooled fluids could increase the effective Reynolds number by a factor of seven or eight.

The feasibility of using this technique of locally high Reynolds number simulation will be discussed and analyzed in the paragraphs that follow.

IV. Development of a High Reynolds Number Simulation Technique

The high Reynolds number simulation technique which is the subject of this study requires the immersion of the structure being tested in an envelope of cool fluid. If the momentum boundary layer develops entirely within the cool fluid layer, the Reynolds number which determines the non-dimensional force coefficient will depend on the properties of the cool fluid.

In particular, the ratio of Reynolds number based on cool fluid properties to Reynolds number based on tunnel fluid properties can be estimated by $Re_c/Re_s \sim v_s/v_c$. For cryogenic temperatures, the ratio v_s/v_c may be as high as seven or eight (see Appendix D).

In order to take advantage of the potential for such an increase in effective Reynolds number it is necessary to study the ways in which the tunnel fluid may interact with the cool fluid.

Three major fluid interactions most significantly impact the development of a Reynolds number simulation technique involving the injection of a cooled gas. These are momentum mixing, thermal mixing, and condensation/icing.

Momentum mixing will occur when fluids moving parallel to each other have different velocities (see fig 2). The shear stress created at the velocity discontinuity will act to smooth the discontinuity and will result in the development of a momentum mixing region.

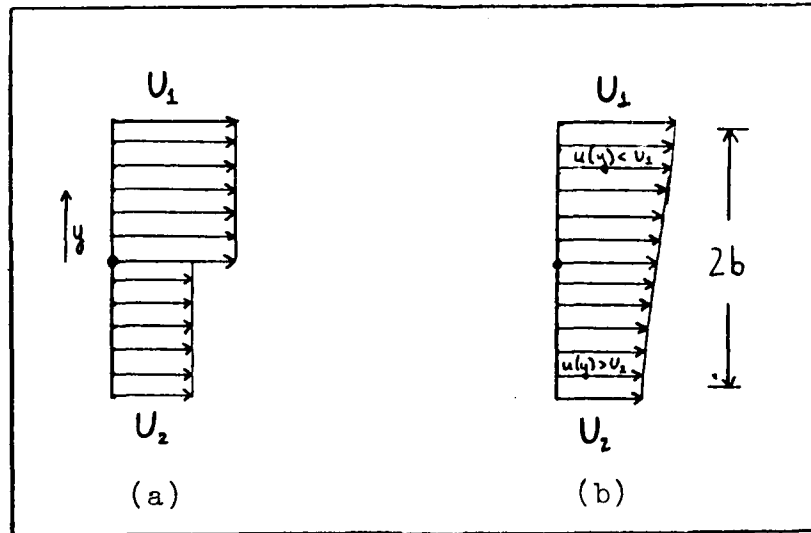


Figure 2. Velocity Profiles for (a) Velocity Discontinuity and (b) Momentum Mixing Region

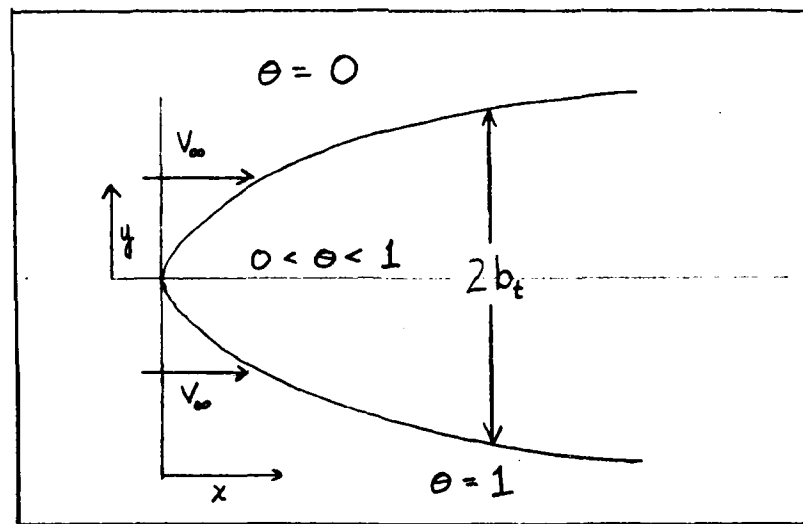


Figure 3. The Thermal Mixing Region

Thermal mixing occurs when a fluid in motion is separated into regions held at different temperatures (see fig 3). The temperature discontinuity will create a thermal gradient and the consequent development of a thermal mixing region.

In the case where a cool fluid comes into contact with atmospheric air, water vapor in the air may condense or solidify. This is the problem of condensation/icing.

Each of these considerations is discussed in detail in the paragraphs which follow.

Momentum Mixing

To determine the effect of a velocity discontinuity between the cool fluid and the tunnel fluid it is convenient to study the flow situation of fig 2. Two fluids, both of which have infinite extent in the y-direction, meet at a point where their velocities are different. The shear stress created at this discontinuity will act to smooth the discontinuity and a momentum mixing region will develop.

This flow situation is discussed in detail by Schlichting (ref 1) and by Yih (ref 5). From ref 1, the velocity profile in the mixing region is given by

$$u(y,t) = \frac{1}{2}(U_1 + U_2) + \frac{1}{2}(U_1 - U_2) \times \{(3/2b)y - (1/2b^3)y^3\} \quad (17)$$

The quantity b which appears in equation 17 is a measure of the size of the momentum mixing region, and Schlichting gives

$$b = \frac{3}{2} \beta^2 (U_1 - U_2) t \quad (18)$$

where β is an empirical constant which depends on the (molecular) mixing length and must be determined from experiment.

The important conclusion to be drawn from equation 18 is the fact that the mixing region will grow with time.

The flow situation for which high Reynolds number simulation is to be attempted is somewhat different from the situation depicted in fig 2. This is because the structure over which the cool fluid is to flow limits the extent of the momentum mixing region.

Equation 18 suggests that if the cool fluid velocity differs from the tunnel free stream velocity, momentum mixing will eventually force the two velocities to be equal in the case where the cool fluid is in the vicinity of a solid boundary.

This equality of velocities is a steady-state condition. The time required to reach steady-state is not easily determined analytically, since such a determination would require advance knowledge of the values for β , U_1 , and U_2 . Some or all of these values can only be determined experimentally.

Nonetheless, it seems reasonable to expect that the time to reach steady-state will be short. This is because the height of the cool fluid layer above the solid boundary will be very small (on the order of magnitude of the momentum boundary layer height) so that it will be readily influenced by the tunnel free stream.

The steady-state assumption should be confirmed experimentally, but it will be made here in order to proceed with the analysis of the proposed high Reynolds number simulation technique.

As a result of the discussion above, the following result is indicated:

"In determining the parameters required for successful high Reynolds number simulation, the free stream velocity of the cool fluid may be taken as equal to the free stream velocity of the wind tunnel."

Thermal Mixing

The success of the high Reynolds number simulation technique under consideration depends on the fact that the kinematic viscosity of a gas decreases with decreasing temperature. It is therefore important to insure that the cool fluid stays cool and is not significantly heated by the much warmer tunnel fluid.

The flow situation of interest is depicted in fig 3.

Appendix B to this report contains a detailed analysis of this situation and develops the solution for the temperature distribution in the thermal mixing region.

Since the energy conducted at the boundary of the thermal mixing region can be balanced by the convection of fluid into the thermal mixing region, a steady-state condition will occur in which the width of the mixing region will not grow with time.

Under the assumptions of 1) steady-state; 2) the temperature mixing region does not effect the velocity field; and 3) gradients in the y-direction are much larger than gradients in the x-direction, the temperature profile in the thermal mixing region is given by

$$\theta(x,y) = \frac{1}{2}\text{erfc}(y/\sqrt{4\alpha x/V_{\infty}}) \quad (y > 0) \quad (19)$$

$$\theta(x,y) = 1 - \frac{1}{2}\text{erfc}(|y|/\sqrt{4\alpha x/V_{\infty}}) \quad (y < 0) \quad (20)$$

where θ is a non-dimensional temperature difference defined by $\theta = (T - T_{\infty})/(T_c - T_{\infty})$.

Of the assumptions used in developing these expressions, the first is certainly reasonable, based on the argument given above. The third assumption is just a restatement of the "boundary layer assumption," and it seems almost self-evident that the thermal mixing region will have a boundary layer characterisitic to it.

The second assumption, however, is not quite so self-evident. It should be noted that Yih (ref 5) makes a

similar assumption in dealing with the temperature distribution created by a pre-heated jet.

If the temperature distribution in the thermal mixing region were to disturb the velocity field, it would create a situation where momentum mixing would occur in the free stream. This mixing would eventually effect the development of the momentum boundary layer and the validity of the Reynolds number simulation technique would be questionable.

Fortunately, results presented below suggest that the size of the thermal mixing region is very small - on the order of magnitude of the momentum boundary layer. It seems reasonable to assume that such a small region will not have a significant effect on the velocity field.

For the sake of establishing the width of the thermal mixing region it is necessary to determine the distance between the isotherms $\theta = 1$ and $\theta = 0$. However, as is characteristic in boundary layer work, the solution for θ indicates that the thermal mixing region extends to infinity in both directions. Therefore, we adopt the convention that the width of the thermal mixing region, $2b_t$, is given by the distance between the isotherms $\theta = 0.99$ and $\theta = 0.01$. If $y = 0$ is taken as the line of symmetry between these isotherms, then b_t is the distance from $y = 0$ to $\theta = 0.99$.

For the purpose of establishing a Reynolds number simulation technique, the extent of the thermal mixing

region into the cool fluid must be studied. In terms of the flow situation depicted in fig 3 this is the region $y < 0$, so equation 20 yields

$$\theta(x,y) = 1 - \frac{1}{2}\text{erfc}(|y|/\sqrt{4\alpha x/V_\infty}) = 0.99 \quad (21)$$

From this, $\text{erfc}(|y|/\sqrt{4\alpha x/V_\infty}) = 0.02$, which yields the result $y/\sqrt{4\alpha x/V_\infty} = -1.65$. Since b_t is given by the distance from the curve $y = 0$ to the curve $\theta = 0.99$, it is clear that

$$y_t = -3.3\sqrt{\alpha x/V_\infty} \quad (22)$$

Equation 22 does not apply exactly to flow over a solid boundary. The fluid streamlines will be deflected away from the boundary due to the action of viscous forces, so the isotherm $\theta = 0.99$ will be deflected away from the boundary as well. Therefore, equation 22 can be taken as a conservative estimate for the extent of the thermal mixing region into the cool fluid layer.

If the thermal mixing region extends into the momentum boundary layer it will effect the boundary layer development. A condition for accurate Reynolds simulation is therefore

"Flow properties must be established to guarantee that the thermal mixing region does not extend into the momentum boundary layer."

Condensation and Icing

From the discussion of the preceding paragraphs it is apparent that it is possible to create a flow situation in which the fluid is kept separated into cool and warm regions. If the warmer fluid contains water vapor (as would be the case for an atmospheric wind tunnel) the water vapor contained within the thermal mixing region can be expected to condense and/or solidify.

This presents a difficulty in attempting to simulate high Reynolds number through injection of a cool gas, since the water and ice particles will be significantly more dense than the surrounding fluid. The motion of these particles will therefore be influenced by gravitational acceleration; this possibility must be accounted for.

Water and ice must be prevented from entering the boundary layer if accurate Reynolds number simulation is to be obtained. Appendix C to this report presents a method for determining the trajectory of a spherical particle of liquid or ice. In the case where the free stream fluid velocity is perpendicular to the gravitational field the equation of motion for the sphere is given by

$$\begin{aligned} u &= V_{\infty} \\ \dot{v} &= -g^* + C_D(3/8r)\hat{v}^2 \text{ if } |g^*| > |C_D(3/8r)\hat{v}^2| \\ \dot{v} &= 0, \text{ otherwise} \end{aligned} \tag{23}$$

subject to the initial condition $v(0) = 0$. The component velocities of the particle tangential and normal to the free stream are denoted by $u(t)$ and $v(t)$, respectively; $\hat{\rho}$ is the ratio of the free stream fluid density to the density of the particle ($\hat{\rho} = \rho_f/\rho_p$); and g^* is the effective acceleration of gravity, taking into account buoyant forces. C_D is the coefficient of drag for a sphere, taken to be

$$\begin{aligned} C_D &= 24/Re & (0 < Re < 0.25) \\ \zeta &= 0.102\xi^2 - 0.894\xi + 1.42 & (0.25 < Re < 2000) \\ C_D &= 0.405 & (2000 < Re < 200,000) \end{aligned} \quad (24)$$

where $\zeta = \log_{10} C_D$, $\xi = \log_{10} Re$, and Re is based on the velocity component v .

With these relationships, equation 23 can be integrated numerically to determine particle trajectory as a function of free stream velocity and sphere diameter. Table 1 gives the distance that a sphere with a diameter of approximately $1/8$ inch can be expected to fall as a function of time. Larger particles will drop more quickly, smaller ones will not fall as fast.

Since the mass fraction of water vapor in the atmosphere is very small, any condensation which occurs in the tunnel can be expected to take the form of a mist. Therefore, large particles of water and ice (on the order of $1/8$ inch, for instance) will not form in the tunnel. Since the

TABLE 1

Distance Fallen by a Spherical Particle of Diameter = 0.01 ft

<u>Time (sec)</u>	<u>Distance (ft)</u>
0.005	0.0004
0.01	0.0016
0.015	0.0036
0.02	0.0064
0.025	0.010
0.03	0.014
0.035	0.020
0.04	0.026
0.045	0.032
0.05	0.040
0.06	0.058
0.07	0.078
0.08	0.10
0.09	0.13
0.1	0.16

results presented in Table 1 and in Appendix C indicate that even relatively large particles will not effect the momentum boundary layer for reasonable values of the free stream tunnel velocity, it is clear that any water vapor mist will be insignificant, as well.

Of course, it is also possible to align a model to be tested in a wind tunnel in such a way as to prevent ice and water from falling towards the boundary layer (i.e., the model could be mounted sideways). In some cases for which the flow geometry is not as simple as the one discussed above, this may be the only way to prevent water and ice from effecting the Reynolds simulation technique.

The conclusion of this discussion on condensation and icing is therefore

"Condensation and icing must be prevented from effecting the momentum boundary layer development either by guaranteeing that fluid free stream velocity is large enough to sweep moisture away from the region of concern, or by choosing an appropriate orientation for the model."

Other Considerations

It is clear that a primary consideration in the development of a successful Reynolds number simulation technique is the necessity to prevent mixing between the warm and the cool fluids. The discussion above outlines ways of dealing with this concern for the flow phenomena

which will effect mixing most significantly.

Three additional considerations may impact mixing, as well. If the cool fluid is not the same as the warm fluid, diffusion will occur between the two fluids. Therefore, it is necessary to select fluids which are "similar enough" (air and nitrogen, for example) to minimize the effect of this diffusion.

The static pressure of the two fluids must be the same in the region of interest. This is not expected to be a significant problem for the technique under consideration, since the cool fluid will be injected through some type of nozzle. When the flow through the nozzle is subsonic, the fluid leaving the nozzle will have a static pressure equal to the static pressure of the tunnel fluid.

The last consideration is the development of density gradients. Gravity will pull a more dense fluid down into a less dense fluid, and, in general, the cool fluid will be more dense than the boundary layer. In the case of an attempt to simulate boundary layer development on the top surface of some object, the density gradient should not be a significant concern since the cool fluid will be below the warm fluid. Across the bottom surface, the density gradient will be significant unless the inertia of the fluid is sufficient to overwhelm the effect of the gravitational force (i.e., when $Gr/Pe^2 \ll 1$). In most other cases the model to be examined will have to be

aligned so that gravity cannot act to pull the cooler fluid into the warmer fluid.

V. High Reynolds Number Simulation: the Flat Plate

This section considers in detail Reynolds number simulation through injection of a cool gas for the case of a flat plate.

The flow situation of interest is illustrated in fig 4. A fluid with uniform velocity, but separated into layers of cool and warm temperature, approaches the leading edge of a flat plate located at position $x = 0$. The x -axis is aligned with the interface between the two temperature regions and is located at a height h above the flat plate. The momentum boundary layer thickness at a point x is denoted by δ , and $2b_t$ gives the width of the thermal mixing region. y_t and y_m are respectively the y -coordinate of the lower boundary of the thermal mixing region (the curve $\theta = 0.99$) and the ordinate of the momentum boundary layer thickness. Both of y_t and y_m are functions of x .

The point at which $y_t = y_m$ has been denoted by x_{crit} , it is at this location that the thermal mixing region will begin to effect the development of the momentum boundary layer.

T_w is the temperature of the flat plate, and for the purpose of this study it is assumed that no heat transfer is taking place at the plate. Therefore, T_w is assumed equal to T_c (or to the adiabatic wall temperature for the case of high speed flow).

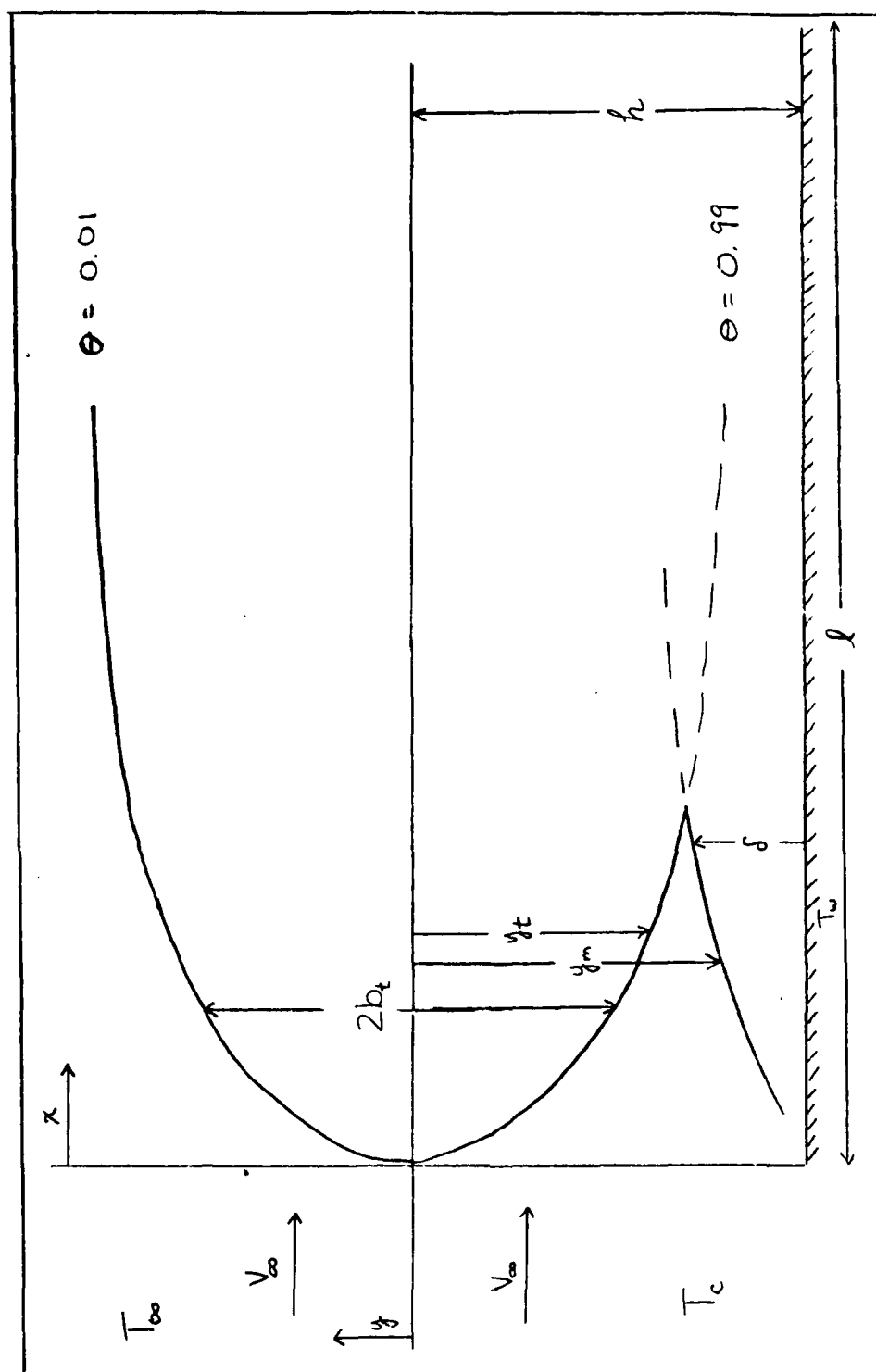


Figure 4. Boundary Layer Development and Cool Fluid Layer Over a Flat Plate

It has been established in previous chapters that a necessary condition for successful Reynolds number simulation prohibits the thermal mixing region from entering the momentum boundary layer.

For a flat plate of length ℓ , this condition requires that $x_{\text{crit}} > \ell$.

For laminar flow, Schlichting (ref 1) gives the boundary layer height, δ , as

$$\delta = 5.0\sqrt{\nu x/V_\infty} \quad (25)$$

In the coordinate reference frame defined by fig 4, this results in the relationship $y_m = -h + \delta$. It has already been established that $y_t = -3.3\sqrt{\alpha x/V_\infty}$. The abscissa for which $y_t = y_m$ is x_{crit} , so

$$-3.3\sqrt{\alpha/V_\infty}\sqrt{x_{\text{crit}}} = -h + 5.0\sqrt{\nu/V_\infty}\sqrt{x_{\text{crit}}} \quad (26)$$

where the values of α and ν are determined at T_c .

Solving equation 26 for x_{crit} yields the result

$$x_{\text{crit}} = (h/L_\ell)^2 \quad (27)$$

where L_ℓ is defined by $L_\ell = 5.0\sqrt{\nu/V_\infty} + 3.3\sqrt{\alpha/V_\infty}$. The condition $x_{\text{crit}} > \ell$ then forces the result

$$(h/L_\ell)^2 > \ell \quad (28)$$

which, as a constraint on h , is written as

$$h > L_\ell \sqrt{x} \quad (29)$$

A similar condition can be derived for the case of turbulent flow by defining the parameter L_t . For turbulent flow over a flat plate, Holman (ref 6) gives

$$\delta = 0.37 \sqrt[5]{\nu/V_\infty} x^{4/5} \quad (30)$$

This value for δ is substituted into the expression $y_m = -h + \delta$ and y_m is equated to y_t , as above. As before, this yields the result

$$x_{\text{crit}} = (h/L_t)^2 \quad (31)$$

where L_t is defined by $L_t = 3.3 \sqrt{\alpha/V_\infty} + 0.37 \sqrt[5]{\nu/V_\infty} x_{\text{crit}}^{3/10}$. Applying the constraint $x_{\text{crit}} > \ell$ and defining L_t in terms of the length ℓ (rather than x_{crit}) yields the condition

$$h > L_t \sqrt{\ell} \quad (32)$$

Equations 29 and 32 are the mathematical expressions of the requirement that the thermal mixing region may not extend into the momentum boundary layer. There are, however, additional constraints on the value of h .

One apparent constraint on h is the requirement that $h > \delta$, to guarantee that the momentum boundary layer is contained within the cool fluid. This condition is automatically satisfied if $h > L\sqrt{\mathcal{L}}$, since $L\sqrt{\mathcal{L}} > \delta$ in all cases.

Another constraint on h is related to the mass rate of flow of the cool fluid, \dot{m} . The mass rate of flow is directly proportional to the cross-sectional area across which the fluid moves. For the case of the flat plate, this cross sectional area is given by $h \times w$, where w is the width of the plate. Therefore,

$$\frac{\dot{m}}{w} = \rho_c V_\infty h \quad (33)$$

where ρ_c is the density of the cool fluid.

Since it has been established above that $h > L\sqrt{\mathcal{L}}$, equation 33 can be cast as a constraint on \dot{m} .

$$\frac{\dot{m}}{w} > \rho_c V_\infty L\sqrt{\mathcal{L}} \quad (34)$$

Therefore, given the value of ρ_c it is possible to determine the required minimum value of \dot{m} .

If the cool fluid can be treated as an ideal gas, then ρ_c can be determined from T_c and p_c . It has already been shown that p_c must equal the static pressure (p_s) of the warm fluid. Therefore, it is assumed that $p_c = p_s$, and then p_s can be determined from the properties of

the warm fluid.

If the flow of the warm fluid can be assumed to be isentropic, the following algorithm can be used to determine p_s :

- 1) Given V_∞ , T_t , and p_t , guess ρ_s .
- 2) Determine $q = \frac{1}{2}\rho V_\infty^2$.
- 3) Let $p_s = p_t - q$
- 4) Form the ratio (p_s/p_t) , and apply the isentropic relationships to determine the ratio (T_s/T_t) :
 - a) Guess a value for γ .
 - b) Solve $T_s = T_t(p_s/p_t)^{(\gamma-1)/\gamma}$
 - c) Determine $\gamma' = \gamma'(T_s)$
 - d) If $\gamma' = \gamma$ then stop, otherwise $\gamma = \gamma'$. Repeat steps b through d.
- 5) Determine $\rho_s' = p_s/(RT_s)$.
- 6) If $\rho_s' = \rho_s$, then stop. Otherwise, let $\rho_s = \rho_s'$ and iterate steps 2 through 6.

In many cases, the assumption that $p_s = p_t$ will be reasonably accurate (see Appendix D), so it may not be necessary to employ the algorithm defined above in order to obtain quick estimates for fluid properties.

Once p_s has been determined, the value of ρ_c can be found from the ideal gas law. Since V_∞ is assumed equal to the free stream tunnel velocity, it is possible to calculate the required mass rate of flow of the cool

fluid from equation 34.

A final constraint on the value of h involves the concern over possible condensation and icing. In the worst case (assuming, again, that there is no momentum mixing occurring) ice or water may form beginning at the point where the two layers of fluid are allowed to exchange energy. In the notation given in fig 4 this is the point $(x,y) = (0,0)$.

A spherical particle formed at location $(0,0)$ and moving with velocity V_{∞} in the x-direction will traverse the length of the plate in a period of time ℓ/V_{∞} . The equations of motion established in Appendix C to this report can be used to determine the distance that a particle of given diameter will fall in the time period ℓ/V_{∞} . The height of the cool fluid layer can then be selected to insure that the particle will not fall into the boundary layer.

In practice, it is probably easiest to select h and \dot{m} based on the criteria given in equations 29 or 32 and 34 and then to check and see if this height is sufficient to prevent water and ice from falling into the boundary layer. If not, h and \dot{m} may be adjusted accordingly.

The results presented above may be simplified somewhat if cruder estimates for the values of the important parameters are acceptable.

From the definition of L_{ℓ} , it is apparent that $L_{\ell}\sqrt{\alpha} \sim 2\delta$, since $\alpha \sim \nu$ for most gases. Therefore, the con-

straint on h can be expressed approximately as

$$h > 2\delta \quad (35)$$

and the constraint on the mass rate of flow becomes

$$\frac{\dot{m}}{w} > 2\rho_c V_\infty \delta \quad (36)$$

Ice or water should not effect the boundary layer development if the condensation does not enter the boundary layer. Since $h \sim 2\delta$, this requires that the distance a solid or liquid particle may fall, y_p , should be less than $h/2$. If viscous forces on the particle are neglected, its equation of motion can be approximated by

$$y_p \approx \frac{1}{2}gt^2 \quad (37)$$

The time t is given by ℓ/V_∞ , and $g = 32 \text{ ft/sec}^2$. In this case, equation 37 becomes

$$y_p \approx 16(\ell/V_\infty)^2 \quad (38)$$

The constraint on y_p is given by $y_p < h/2$, so $16(\ell/V_\infty)^2 < \frac{1}{2}L_\ell\sqrt{\mathcal{L}}$, or

$$32(\ell/V_\infty)^2 < L_\ell\sqrt{\mathcal{L}} \quad (39)$$

which can be written in terms of δ as

$$16(\ell/V_\infty)^2 < \delta \quad (40)$$

For turbulent flows, the momentum boundary layer thickness is generally much greater than the depth of the thermal mixing region, so $L_t \sqrt{\mathcal{L}} \sim \delta$. In this case, the constraints on h and \dot{m} can be approximated by

$$h > \delta \quad (41)$$

$$\frac{\dot{m}}{\omega} > \rho_c V_\infty \delta \quad (42)$$

Direct application of equations 41 and 42 would result in the constraint $y_p < 0$, which is clearly unacceptable. It would be convenient to develop a relationship similar to equation 39 for the case of turbulent flows. It can be argued that the high energy characteristic of turbulent flows will tend to overwhelm the effects of condensation in the boundary layer, so some penetration of the momentum boundary layer by water or ice may be tolerated. Guided by the form of equation 39, the constraint on y_p is again chosen to be $y_p < h/2$ to yield

$$32(\ell/V_\infty)^2 < L_t \sqrt{\mathcal{L}} \quad (43)$$

In summary, the constraints which determine the necessary parametric values for successful Reynolds number

simulation are:

1. $h > L\sqrt{\mathcal{L}}$
2. $\frac{\dot{m}}{w} > \rho_c V_\infty L\sqrt{\mathcal{L}}$
3. $32(\ell/V_\infty)^2 < L\sqrt{\mathcal{L}}$

Some results regarding the parameter L which appears in each of these expressions are developed in Appendix B to this report.

VI. A Proposed Experimental Design

For the purpose of verifying some aspects of the theoretical development presented in this study, the experimental apparatus depicted in fig 5 has been designed and built with the assistance of the AFIT shop.

The apparatus is basically a thick flat plate made of aluminum. An ellipsoidal nose of plexiglas is designed to fit on the leading edge of the plate, the cool fluid is to be injected through this nose and across the plate.

The plate is one inch thick and is constructed from two one-half inch thick sheets of aluminum which are bolted together. Three small channels lead from a manifold located near the leading edge of the plate to openings at the trailing edge so that coolant may be fed to the inside of the plate.

The necessity of these cooling channels is demonstrated by a lumped-capacity analysis of the plate. In a lumped-capacity analysis, the temperature of the aluminum is assumed to be uniform and its dependence on time is given by

$$\frac{T - T_{\infty}}{T_0 - T_{\infty}} = \exp\{-(hs/\rho c_p V)t\} \quad (44)$$

where T_0 is the initial temperature of the plate and T_{∞} is the temperature of the free stream fluid around the

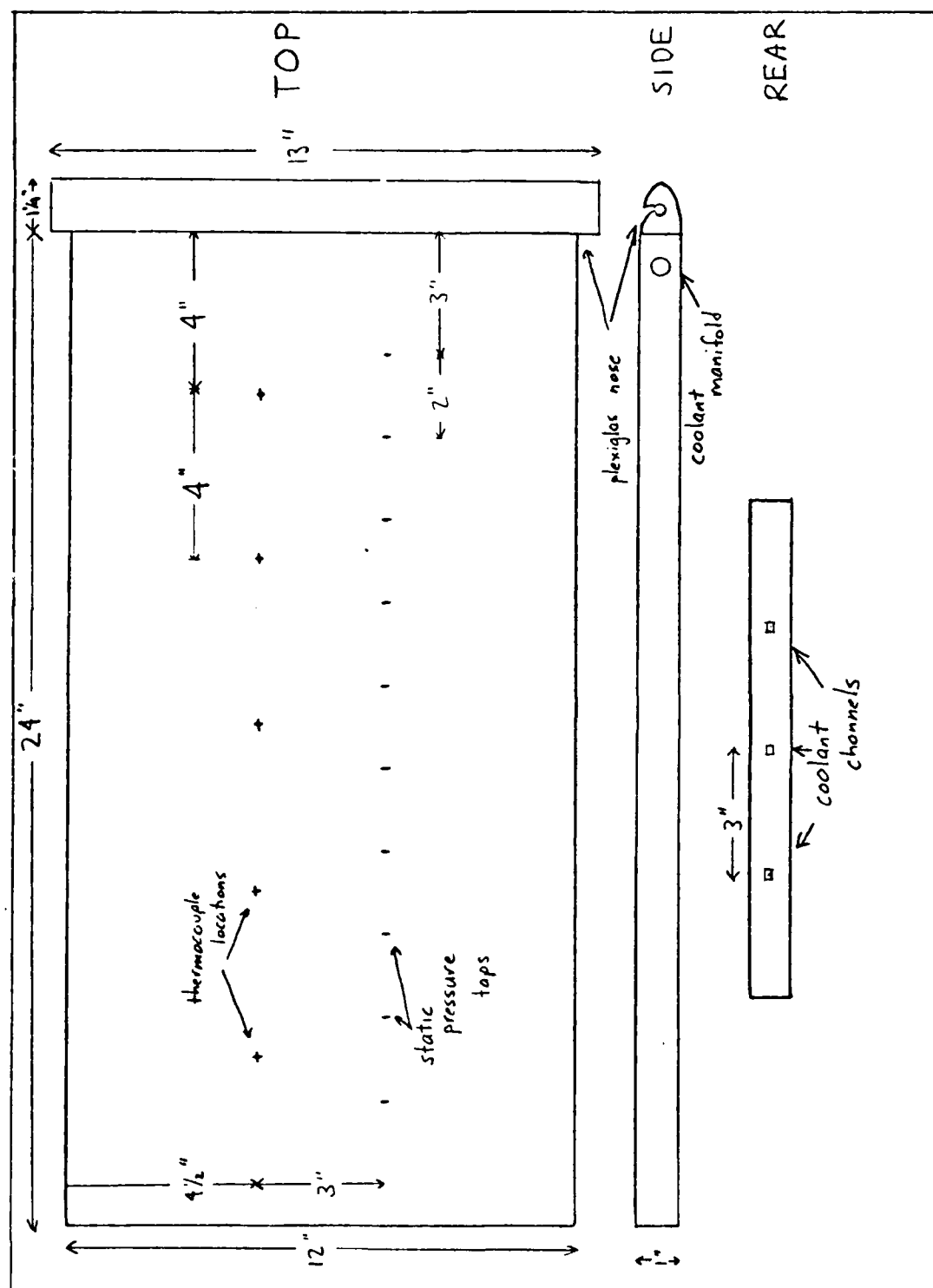


Figure 5. Detail of Experimental Design

plate, V is the volume of the plate and S is its surface area, h is the convective heat transfer coefficient, and ρ and c_p are the density and specific heat, respectively, of the plate.

Equation 44 is a good approximation for $T(t)$ when the Biot number, $Bi = \frac{hV}{kS}$, is much less than one. For a flat plate with thickness a , the Biot number is given by $Bi = \frac{ha}{2k}$.

The thermal conductivity of aluminum can be taken to be 240 W/m-K and the value of the heat transfer coefficient can be obtained from the empirical relationship $\frac{hx}{k_a} = Nu_x = 0.0296 Re^{4/5} Pr^{1/3}$ for turbulent flow (ref 6).

For the plate under consideration, $\ell = 2$ ft, and k_a , the thermal conductivity of air, can be taken to be 0.03 W/m-K.

With these values, and for h evaluated at $x = \ell$, the value of Bi can be obtained as a function of free stream fluid velocity. In the present case, $0.0015 < Bi < 0.0168$ for $15 \text{ m/sec} < V_\infty < 305 \text{ m/sec}$, so a lumped capacity analysis is justified.

Denoting by t_c the quantity $(\rho c_p V / hS)$ found in equation 44, the time to reach steady-state temperature can be chosen (by convention) to be $3t_c$. For the velocity range noted above, this yields $660 \text{ sec} > t_c > 60 \text{ sec}$. These values indicate an unacceptably long period of time for the establishment of steady-state conditions. For this reason (and because it has been assumed that there

is no heat transfer at the plate) it is necessary to provide a means of cooling the plate.

The width of the plate is one foot so that it may be tested in the AFIT 14-inch wind tunnel. Ten static pressure taps are located 4.5 in from one side of the plate and are evenly spaced down its length. Five copper-constantan thermocouples are situated 4.5 in from the other side of the plate.

The plexiglas nose is designed to have a uniformly varying radius of curvature so that the fluid moving over it will not experience an abrupt change in radius of curvature as it reaches the leading edge of the plate. The equation for the nose is given by $(\frac{x}{a})^n + (\frac{y}{b})^n = 1$ with $a = 1.25$ in, $b = 0.5$ in, and $n = 2.5$. The nose is 13 in wide and has a 0.5 in hole drilled through it. Cold nitrogen can be fed to this channel as either a liquid or as a gas.

A slot of 0.03 in is cut at the top of the channel at the shoulder point of the ellipsoid (see fig 5). The top of the nose is cut smoothly to meet the slot, and is designed to help turn the nitrogen so that it will flow across the plate and parallel to the tunnel free stream.

The nose is designed with a slot that fits a groove on the leading edge of the aluminum plate. This allows the possibility of testing a variety of different nozzle designs by simply interchanging plexiglas noses.

Cryogenic nitrogen is chosen for use as the cool fluid due to its similarity to atmospheric air (i.e.,

atmospheric air is approximately 78% nitrogen). As noted before, the nitrogen can be introduced into the nose as either a liquid or a gas; the choice of phase is dependent on the desired values for T_c and \dot{m} .

Use of gaseous nitrogen allows control over the pressure inside the nozzle, and therefore \dot{m} can be easily controlled. A disadvantage to the use of gaseous nitrogen, however, is the difficulty in controlling and monitoring its temperature.

The use of liquid nitrogen is constrained by a limited ability to control \dot{m} - the mass rate of flow will be primarily dependent on the rate of evaporation of the nitrogen within the nozzle. This rate can be controlled to a limited degree by providing a means of heating the plexiglas nose.

Liquid nitrogen could also be boiled externally, and then fed to the nose as a gas. This external boiling would allow greater control over \dot{m} , and T_c could be controlled by providing sufficient insulation for the fluid.

For the purpose of studying the theoretical predictions of this paper there is an additional advantage to the use of liquid nitrogen. Since the temperature inside the nozzle will be the boiling temperature of nitrogen (~ 140 R) and since the expansion through the nozzle will be isenthalpic (a Joule-Thomson expansion), the temperature of the gas leaving the nozzle will be known.

Measurement of the flow properties presents a chal-

lenge because of the very low temperatures involved. Dynamic pressure and temperature must be measured simultaneously in order to determine the velocity profile in the boundary layer. The dynamic pressure, q , is equal to $\frac{1}{2}\rho v^2$, and the temperature is required to evaluate ρ . Temperature readings are also required in order to compare the predicted extent of the thermal mixing region with measured data.

For accurate measurements with reasonable response time, hot wire or hot film anemometers may be used. It should be noted that hot wire (film) probes are calibrated for a particular temperature; if they are not calibrated at T_c a correction must be made for this. This is discussed in some detail in ref 7, and ref 8 gives a method for using hot wire anemometers to measure both temperature and dynamic pressure under very controlled conditions.

For a quick check on the predictions made in this paper it may suffice to measure q with a pitot probe and to take total temperature readings with a thermocouple. If the flow speed is not too high, the total temperature will be an adequate approximation to the static temperature of the fluid.

Care must be taken at the beginning of the test run to insure that the surface of the plate does not ice - the nitrogen must be swept quickly across the plate to displace the air before water vapor in the air can condense.

This difficulty can be eliminated altogether if warm nitrogen is used to sweep the atmospheric air from the surface of the plate before the cool nitrogen is introduced.

The analyses contained in Appendices D and E to this report indicate that very high mass rates of flow for cool nitrogen are required for high Reynolds number simulation. The experimental apparatus described above will not be able to handle those requirements, due primarily to the small size of the nozzle through which the nitrogen is being injected.

Nonetheless, this apparatus can be used to provide preliminary verification of certain aspects of the theoretical development given in this paper. In particular, experimental data is required to more accurately determine the extent of the thermal mixing region, the effect of any momentum mixing which may occur, and the impact (if any) of condensation or icing on momentum boundary layer development.

VII. Conclusions and Recommendations

This paper has analyzed the potential for high Reynolds number simulation in a wind tunnel through use of a cool gas to envelop the momentum boundary layer. If this technique can be used, effective Reynolds number simulation can theoretically be increased by a factor of seven or eight.

To be successful, the flow of the warm tunnel air must not interfere with the locally cool fluid flow. For the case of a flat plate, it has been shown that this condition will be met when:

1. $h > L\sqrt{x}$
2. $\dot{m}/w > \rho_c V_\infty L\sqrt{x}$
3. $32(\ell/V_\infty)^2 < L\sqrt{x}$

The conditions defined above are based in part on certain assumptions - in particular, that the cool fluid free stream velocity is equal to the tunnel free stream velocity, and that condensation and icing are not significant concerns if the condensation does not penetrate too far into the boundary layer.

Under these circumstances, high Reynolds number simulation can theoretically be achieved if the constraints 1 - 3 noted above are satisfied.

In practice, the required value of \dot{m} for high Rey-

nolds number simulation will be very large (on the order of 0.5 to 1.0 lb_m/sec for the example discussed in this paper). Therefore, it may not be a simple matter to apply the theoretical constraints to a situation of interest.

Recommendations for Further Study

Further study in the following areas will add significantly to the development of a successful high Reynolds number simulation technique:

1. The experimental apparatus discussed in Chapter VI should be used to verify the assumptions noted above.
2. The development which has been presented for the case of a flat plate should be extended to structures of arbitrary shape.
3. Various means of injecting the cool fluid in order to provide the mass rates of flow required for successful high Reynolds number simulation should be investigated.

Bibliography

1. Schlichting, H., Boundary Layer Theory, 7th ed., McGraw-Hill Book Co., New York 1979.
2. National Aeronautics and Space Administration, Cryogenic Wind Tunnel Models, CP-2262. Hampton, Virginia: NASA Langley Research Center, 5-9 May 1982.
3. Lan, Chuan-Tau Edward and Jan Roskam, Airplane Aerodynamics and Performance, Roskam Aviation and Engineering Corp., Ottawa, Kansas, 1981.
4. Luchuk, W., unpublished correspondence, Arvin Calspan Field Services, Inc.
5. Yih, Chia-Shun, Fluid Mechanics, West River Press, Ann Arbor, Michigan, 1977.
6. Holman, J., Heat Transfer, 5th ed., McGraw-Hill Book Co., New York, 1981.
7. Arya, S.P.S. and E.J. Plate, "Hot Wire Measurements in Non-Isothermal Flow," Instruments and Control Systems, Vol 42 No 3, March 1969.
8. Artt, D.W. and A. Brown, "The Simultaneous Measurement of Velocity and Temperature," Journal of Physics E: Scientific Instruments, Vol 4 No 1, Jan 1971.
9. Aris, Rutherford, Vectors, Tensors, and the Basic Equations of Fluid Mechanics, Prentice-Hall, Inc., Englewood Cliffs, NJ, 1962.
10. Sokolnikoff, I.S., Tensor Analysis Theory and Applications to Geometry and Mechanics of Continua, 2nd ed., John Wiley and Sons, New York, 1964, 314-330.
11. Bird, R. Byron, W.E. Stewart and E.N. Lightfoot, Transport Phenomena, John Wiley and Sons, Inc., New York, 1960, 83-91 and 715-742.
12. White, Frank M., Viscous Fluid Flow, McGraw-Hill Book Co., New York, 1974.

13. Erdélyi, A., W. Magnus, F. Oberhettinger, and F. Tricomi (The Bateman Manuscript Project), Tables of Integral Transforms, Vol 1, McGraw-Hill Book Co., New York, 1954.
14. Kays, W.M., Convective Heat and Mass Transfer, McGraw-Hill Book Co., New York, 1966.
15. Roskenow, W.M. and J.P. Hartnett (editors), Handbook of Heat Transfer, McGraw-Hill Book Co., New York, 1973.

Appendix A. The Governing Equations for Viscous Fluid Flow

The purpose of this appendix is to develop in detail the equations presented in Chapter II which model the behavior of viscous fluids.

The Continuity Equation

The mass contained in a control volume, Ω , at any time, t , is equal to the volume of the region Ω multiplied by the average density, $\bar{\rho}(t)$, of the mass contained within Ω at that time. In general, mass may be transported across the boundary of the control volume, $\partial\Omega$. The excess of the mass entering the region over the mass leaving the region must remain stored within Ω .

The rate of mass transfer at some point on $\partial\Omega$ is given by $(\rho V_n)^* \times (\Delta s)$, where Δs is an element of surface area on $\partial\Omega$, V_n is the component of the fluid velocity perpendicular to the element Δs , and $(\rho V_n)^*$ is the average value of ρV_n taken over Δs . For convention, ρV_n is taken as positive going into Ω , and negative otherwise.

If no mass is created within Ω , the mass contained within the region at time $t+\Delta t$ must be equal to the mass stored at time t plus the net influx of mass into the region over the time Δt . Mathematically, this can be expressed as

$$\tilde{\rho}(t+\Delta t) \times \text{Vol}(\Omega) = \tilde{\rho}(t) \times \text{Vol}(\Omega) + (\rho V_n)^* \times \text{Area}(\partial\Omega) \times \Delta t \quad (\text{A.1})$$

Dividing through by Δt , rearranging, and taking the limit as $\Delta t \rightarrow 0$, this becomes

$$\frac{\partial \tilde{\rho}}{\partial t} \times \text{Vol}(\Omega) = (\rho V_n)^* \times \text{Area}(\partial\Omega) \quad (\text{A.2})$$

As $\text{Vol}(\Omega) \rightarrow d\text{Vol}$ so $\text{Area}(\partial\Omega) \rightarrow ds$, and average properties taken over the volume Ω approach the average values taken over $\partial\Omega$. Furthermore, ρV_n can be rewritten as $-(\rho \bar{v} \cdot \hat{n})$, where \hat{n} is taken to be the outward pointing normal associated with ds . A fundamental result from the calculus of vectors and tensors yields $\rho \bar{v} \cdot \hat{n} ds = \nabla \cdot \rho \bar{v} d\text{Vol}$ (ref 9). Applying these results to equation A.2 gives

$$\frac{\partial \rho}{\partial t} = - (\nabla \cdot \rho \bar{v}) \quad (\text{A.3})$$

This is the Continuity Equation, and it is more frequently written as

$$\begin{aligned} \frac{\partial \rho}{\partial t} + (\nabla \cdot \rho \bar{v}) &= 0, \text{ or equivalently as} \\ \frac{D\rho}{Dt} + \rho(\nabla \cdot \bar{v}) &= 0 \end{aligned} \quad (\text{A.4})$$

In many applications, it is reasonable to take ρ as essentially constant, in which case $\frac{D\rho}{Dt}$ is identically zero and the Continuity Equation reduces to

$$(\nabla \cdot \bar{v}) = 0 \quad (A.5)$$

The Momentum Equation

The momentum contained within a fixed region in space (Ω) will change with time due to the addition of mass to Ω and due to forces which act on the mass contained in the control volume. Considering the limiting case as $\text{Vol}(\Omega) \rightarrow 0$ this can be expressed mathematically as

$$(\rho \bar{v})(t+\Delta t) d\text{Vol} = \rho \bar{v}(t) d\text{Vol} + (\rho \bar{v} V_n) ds \Delta t + (\bar{\sigma} ds) \Delta t + (\rho \bar{f} d\text{Vol}) \Delta t \quad (A.6)$$

where \bar{f} denotes the body force per unit mass acting on the fluid contained within Ω and $\bar{\sigma}$ is the force due to stress acting on the surface $\partial\Omega$. It is clear that $\bar{\sigma}$ depends on the state of stress at ds as well as on the orientation of the elemental surface area. This dependence is expressed as $\bar{\sigma} = \bar{\sigma} \cdot \hat{n}$, where $\bar{\sigma}$ is the stress tensor (ref 10).

Noting that $\rho \bar{v} V_n = -\rho \bar{v} \bar{v} \cdot \hat{n}$, dividing through the equation above by Δt , and taking the limit yields

$$d\text{Vol} \frac{\partial(\rho \bar{v})}{\partial t} = -\rho \bar{v} \bar{v} \cdot \hat{n} ds + \bar{\sigma} \cdot \hat{n} ds + \rho \bar{f} d\text{Vol} \quad (A.7)$$

At equilibrium, application of the law of conservation of angular momentum demonstrates that $\bar{\sigma}$ is symmetric. Since

$\bar{v} \bar{v}$ is the outer product of a vector with itself, $\bar{v} \bar{v}$ is also symmetric, and so $\bar{\sigma} \cdot \hat{n} \, ds = \nabla \cdot \bar{\sigma} \, dVol$ and $\rho \bar{v} \bar{v} \cdot \hat{n} \, ds = \nabla \cdot (\rho \bar{v} \bar{v}) \, dVol$. The term $\nabla \cdot (\rho \bar{v} \bar{v})$ can be expanded as $(\nabla \cdot \rho \bar{v}) \bar{v} + \rho (\bar{v} \cdot \nabla \bar{v})$.¹ The continuity equation gives $\nabla \cdot \rho \bar{v} = -\frac{\partial \rho}{\partial t}$, so the equation above reduces to

$$\frac{\partial(\rho \bar{v})}{\partial t} - \rho (\bar{v} \cdot \nabla \bar{v}) = \nabla \cdot \bar{\sigma} + \rho \bar{f} \quad (A.8)$$

Expanding the first term on the left side of this equation and simplifying yields

$$\begin{aligned} \rho \left(\frac{\partial \bar{v}}{\partial t} + \bar{v} \cdot \nabla \bar{v} \right) &= \nabla \cdot \bar{\sigma} + \rho \bar{f}, \text{ which is equivalent to} \\ \rho \frac{D \bar{v}}{Dt} &= \nabla \cdot \bar{\sigma} + \rho \bar{f} \end{aligned} \quad (A.9)$$

Equation A.9 is Cauchy's equation of motion. The Navier-Stokes equations are developed from equation A.9 by determining the relationship between the stress tensor and the rate of deformation of the fluid contained within Ω . It is convenient to separate the stress tensor into components perpendicular to $\partial\Omega$ (pressure) and tangential to $\partial\Omega$ (shear stress). Since pressure is taken as constant over $\partial\Omega$ for Ω sufficiently small, we can write $\bar{\sigma} = -p\bar{I} + \bar{\tau}$, where \bar{I} is the identity tensor.

If the fluid is assumed to be Newtonian, the components

¹ Note that $\bar{v} \cdot \nabla \bar{v} \neq (\bar{v} \cdot \nabla) \bar{v}$ in general, unless a Cartesian coordinate system is used. A general identity is $\bar{v} \cdot \nabla \bar{v} = \Delta \text{grad}(\bar{v} \cdot \bar{v}) - (\bar{v} \times (\nabla \times \bar{v}))$

of stress are linearly dependent on the rates of deformation of the fluid. It can be shown (refs 1 and 11) that this relationship is given by $\bar{\tau} = \lambda(\nabla \cdot \bar{v})\bar{I} + \mu(\nabla \bar{v} + \text{grad } \bar{v})$.

Substituting this expression for $\bar{\tau}$ into equation A.9 and making use of the identity $\nabla \cdot a\bar{I} = \nabla a$ (a is a scalar) results in the Navier-Stokes equations:

$$\rho \frac{D\bar{v}}{Dt} = -\nabla p + \nabla(\lambda \nabla \cdot \bar{v}) + \nabla \cdot \mu(\nabla \bar{v} + \text{grad } \bar{v}) + \rho \bar{f} \quad (\text{A.10})$$

As a consequence of Stokes' Hypothesis (ref 12), the parameters μ and λ are assumed related by the equation $3\lambda + 2\mu = 0$.

If the coefficient of viscosity, μ , is assumed constant, and if the function \bar{v} is twice continuously differentiable so that the order of differentiation may be interchanged (resulting in the identity $\nabla \cdot \text{grad } \bar{v} = \nabla(\nabla \cdot \bar{v})$), then equation A.10 reduces to

$$\rho \frac{D\bar{v}}{Dt} = -\nabla p + \mu \nabla^2 \bar{v} + \frac{1}{3}\mu \nabla(\nabla \cdot \bar{v}) + \rho \bar{f} \quad (\text{A.11})$$

In the case of incompressible flow, the Continuity Equation gives $\nabla \cdot \bar{v} = 0$, and when body forces are neglected

¹ $\nabla^2 \bar{v} \equiv \nabla \cdot \nabla \bar{v} \neq (\nabla \cdot \nabla) \bar{v}$, except in Cartesian coordinate systems.
Alternately, $\nabla^2 \bar{v} = \nabla(\nabla \cdot \bar{v}) - (\nabla \times (\nabla \times \bar{v}))$

ted, the Momentum Equation takes the form

$$\rho \frac{D\bar{v}}{Dt} = -\nabla p + \mu \nabla^2 \bar{v} \quad (A.12)$$

The Energy Equation

The energy contained within a fixed region in space (Ω) will change with time due to addition of mass to the control volume, heat added to the control volume, and work done on the control volume. Considering the limiting case as $\text{Vol}(\Omega) \rightarrow 0$, this is expressed as

$$\begin{aligned} \rho E(t+\Delta t) d\text{Vol} = & \rho E(t) d\text{Vol} + (\bar{\sigma} \cdot \bar{v}) \Delta t ds + \rho \bar{f} \cdot \bar{v} \Delta t ds \\ & + q_n \Delta t ds + (\rho \bar{v} E)_n \Delta t ds \end{aligned} \quad (A.13)$$

where E is the energy per unit mass and q_n is the component of heat flux perpendicular to ds and directed into Ω . By noting that $\bar{\sigma} = \bar{\sigma} \cdot \hat{n}$, $q_n = -\bar{q} \cdot \hat{n}$, and $(\rho \bar{v} E)_n = -\rho \bar{v} E \cdot \hat{n}$, this becomes

$$\begin{aligned} \rho E(t+\Delta t) d\text{Vol} = & \rho E(t) d\text{Vol} + (\bar{\sigma} \cdot \bar{v}) \cdot \hat{n} \Delta t ds + \rho \bar{f} \cdot \bar{v} \Delta t ds \\ & - \bar{q} \cdot \hat{n} \Delta t ds - \rho \bar{v} E \cdot \hat{n} \Delta t ds \end{aligned} \quad (A.14)$$

Applying the identity $\bar{a} \cdot \hat{n} ds = \nabla \cdot \bar{a} d\text{Vol}$ for any vector \bar{a} , dividing through by Δt , and taking the limit as $\Delta t \rightarrow 0$, the energy equation takes the form

$$\frac{\partial}{\partial t}(\rho E) = \nabla \cdot (\bar{\bar{\sigma}} \cdot \bar{v}) + \rho \bar{f} \cdot \bar{v} - \nabla \cdot \bar{q} - \nabla \cdot \rho \bar{v} E \quad (A.15)$$

Applying the vector identity $\nabla \cdot c\bar{a} = c(\nabla \cdot \bar{a}) + \bar{a} \cdot \nabla c$ to the last term of this equation, expanding the derivative on the left, and noting that $\frac{\partial \rho}{\partial t} = -(\nabla \cdot \rho \bar{v})$ from continuity, the energy equation takes the form

$$\rho \frac{DE}{Dt} = \nabla \cdot (\bar{\bar{\sigma}} \cdot \bar{v}) + \rho \bar{f} \cdot \bar{v} - \nabla \cdot \bar{q} \quad (A.16)$$

This is the total energy equation. In the case where changes in potential and chemical energy can be neglected, E can be taken to be $(e + \frac{1}{2}\bar{v} \cdot \bar{v})$ where e is the internal energy per unit mass and $\frac{1}{2}\bar{v} \cdot \bar{v}$ is the kinetic energy per unit mass.

When the momentum equation (eqn A.9) is dotted with the velocity vector, the result is

$$\rho \frac{D\bar{v}}{Dt} \cdot \bar{v} = \nabla \cdot \bar{\bar{\sigma}} \cdot \bar{v} + \rho \bar{f} \cdot \bar{v} \quad (A.17)$$

When this is subtracted from the total energy equation (making use of the identity $\nabla \cdot (\bar{\bar{\sigma}} \cdot \bar{v}) = \nabla \cdot \bar{\bar{\sigma}} \cdot \bar{v} + \bar{\bar{\sigma}} : \nabla \bar{v}$), the result is the thermal energy equation:

$$\rho \frac{De}{Dt} = \bar{\bar{\sigma}} : \nabla \bar{v} - \nabla \cdot \bar{q} \quad (A.18)$$

Substitution of the expression for $\bar{\bar{\sigma}}$ given earlier

results in the following form of the thermal energy equation:

$$\begin{aligned} \rho \frac{De}{Dt} &= -p \nabla \cdot \bar{v} - \nabla \cdot \bar{q} + \Phi \\ \Phi &= \lambda (\nabla \cdot \bar{v})^2 + 2\mu (\epsilon_{11}^2 + \epsilon_{22}^2 + \epsilon_{33}^2) + 4\mu (\epsilon_{12}^2 + \epsilon_{23}^2 + \epsilon_{31}^2) \end{aligned} \quad (A.19)$$

where the ϵ 's are the components of the rate of strain tensor (see ref 1 and 10). Φ represents the dissipation of energy due to viscous effects; in many practical applications it is assumed to be negligible.

In terms of enthalpy ($h = e + p/\rho$), and when viscous dissipation is negligible, the thermal energy equation becomes

$$\rho \frac{Dh}{Dt} = \frac{Dp}{Dt} - \nabla \cdot \bar{q} \quad (A.20)$$

For a perfect gas, $Dh = c_p DT$. If \bar{q} is linearly dependent on the gradient of temperature, the thermal energy equation takes the form

$$\rho c_p \frac{DT}{Dt} = \frac{Dp}{Dt} + \nabla \cdot (k \nabla T) \quad (\bar{q} = -k \nabla T) \quad (A.21)$$

For the case of constant properties and pressure, this reduces to the familiar form

$$\frac{DT}{Dt} = \alpha \nabla^2 T \quad (\alpha = k/\rho c_p) \quad (A.22)$$

Appendix B. The Thermal Mixing Region

Consider the flow situation depicted in figure B.1. A fluid is moving in the x-coordinate direction with velocity V_{∞} . The fluid below the x-axis is initially at temperature T_c and the fluid above the x-axis is held at T_{∞} . Diffusion of enthalpy (or temperature, for the constant property case) is prohibited until the fluid reaches the position $x = 0$.

At this point, a temperature mixing region will begin to develop and grow until the diffusion (conduction) of energy is balanced by convection. This balance is the condition for steady-state.

The extent of the temperature mixing region must be determined. Clearly, the width of the mixing region, $2b$, can be expected to grow with increased distance from the point where mixing begins. As a first cut approximation, one might expect isotherms as plotted in the x-y plane to have the form $y = kx$ (straight lines). As the mixing region grows in the downstream direction, however, the heat flux at an isotherm will decrease. This suggests that the rate of growth of the temperature mixing region should decrease with increased distance from the initial point of mixing. A more appropriate relationship for isotherms might therefore be assumed as $y = kx^{(1/n)}$.

For the constant property case, the energy equation is equation A.22:

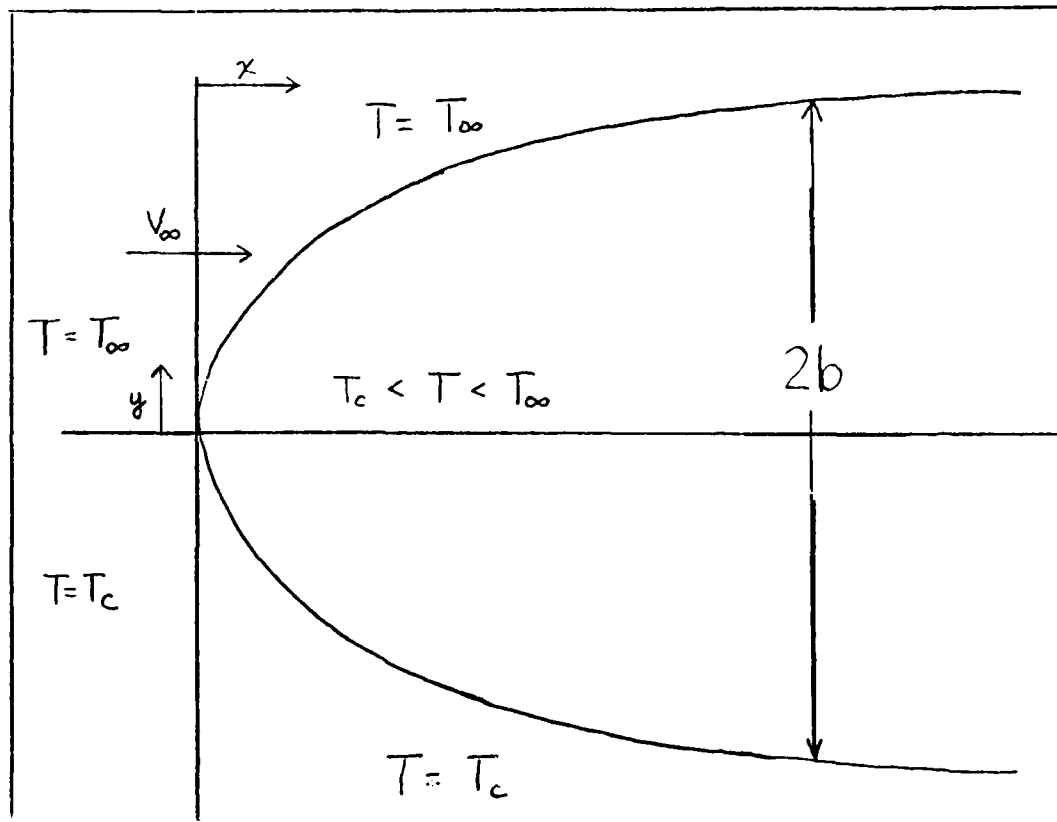


Figure B.1. Development of the Thermal Mixing Region

$$\frac{DT}{Dt} = \alpha \nabla^2 T \quad (B.1)$$

which is expanded in terms of two-dimensional Cartesian coordinates as

$$\frac{\partial T}{\partial t} + u \frac{\partial T}{\partial x} + v \frac{\partial T}{\partial y} = \left(\frac{\partial^2 T}{\partial x^2} + \frac{\partial^2 T}{\partial y^2} \right) \quad (B.2)$$

The following assumptions will be used in reducing equation B.2:

- a) steady-state conditions exist, so that $\frac{\partial T}{\partial t} = 0$.
- b) The momentum (velocity) field is unaffected by the temperature mixing region, so that $u = V_\infty$ and $v = 0$.
- c) Gradients in the y-direction are much larger than gradients in the x-direction so that $\frac{\partial^2 T}{\partial x^2}$ is negligible compared to $\frac{\partial^2 T}{\partial y^2}$ (the "boundary layer assumption").

Under these conditions, equation B.2 becomes

$$\frac{\partial T}{\partial x} = \frac{\alpha}{V_\infty} \left(\frac{\partial^2 T}{\partial y^2} \right) \quad (B.3)$$

It is generally convenient to non-dimensionalize the variable of interest in equations such as B.3, and therefore a non-dimensional temperature difference, θ , is defined as

$$\theta = \frac{T - T_{\infty}}{T_c - T_{\infty}} \quad (\text{B.4})$$

and equation B.3 becomes

$$\frac{\partial \theta}{\partial x} = \frac{\alpha}{V_{\infty}} \left(\frac{\partial^2 \theta}{\partial y^2} \right) \quad (\text{B.5})$$

The boundary conditions which apply to the steady-state temperature field are:

$$\begin{aligned} \text{for } y > 0, \quad T(0,y) &= T_{\infty} \\ \text{for } y < 0, \quad T(0,y) &= T_c \\ \text{as } y \rightarrow \infty, \quad T(x,y) &\rightarrow T_{\infty} \\ \text{as } y \rightarrow -\infty, \quad T(x,y) &\rightarrow T_c \\ T(x,0^+) &= T(x,0^-) = \frac{1}{2}(T_c + T_{\infty}) \end{aligned} \quad (\text{B.6})$$

Under the transformation to the non-dimensional variable θ these conditions become:

$$\begin{aligned} \text{for } y > 0, \quad \theta(0,y) &= 0 \\ \text{for } y < 0, \quad \theta(0,y) &= 1 \\ \text{as } y \rightarrow \infty, \quad \theta(x,y) &\rightarrow 0 \\ \text{as } y \rightarrow -\infty, \quad \theta(x,y) &\rightarrow 1 \\ \theta(x,0^+) &= \theta(x,0^-) = \frac{1}{2} \end{aligned} \quad (\text{B.7})$$

The problem described by figure B.1 is therefore defined by equation B.5 and boundary conditions B.7 Two

possible methods of solution are convenient for this problem: the use of Laplace transforms on the x-variable to obtain an ordinary differential equation in the Laplace domain, or the determination of a similarity transformation $(x,y) \rightarrow (\eta)$ to convert equation B.5 to an ordinary differential equation in η . Both of these methods are examined below.

The Laplace Transform Method

Use of the Laplace transform in this case is motivated by the fact that the energy equation contains the Laplacian, $\nabla^2 T$. The existence of exhaustive compilation of tables of Laplace transforms and inverse Laplace transforms suggests that a solution of the transformed, ordinary differential equation will be readily invertible, resulting in a closed-form solution in the original (x,y) space.

Denoting by $\bar{\theta}$ the Laplace transform of θ (and transforming on the variable x), then

$$\bar{\theta}(s,y) = \int_0^{\infty} e^{-sx} \theta(x,y) dx \quad (B.8)$$

Applying the transformation to equation B.5 and boundary conditions B.7 yields the following ordinary differential equation and associated boundary conditions:

$$\begin{aligned}
\text{for } y > 0: \quad s\tilde{\theta} &= \frac{\alpha}{V_{\infty}} \left(\frac{d^2 \tilde{\theta}}{dy^2} \right) \\
&\text{as } y \rightarrow \infty, \tilde{\theta} \rightarrow 0 \\
\tilde{\theta}(s, 0^+) &= 1/(2s) \\
\text{for } y < 0: \quad s\tilde{\theta} &= \frac{\alpha}{V_{\infty}} \left(\frac{d^2 \tilde{\theta}}{dy^2} \right) + 1 \\
&\text{as } y \rightarrow -\infty, \tilde{\theta} \rightarrow 1/s \\
\tilde{\theta}(s, 0^-) &= 1/(2s)
\end{aligned} \tag{B.9}$$

The solution for the case $y > 0$ must be established separately from the solution for the case $y < 0$ due to the fact that $\theta(x, y)$ has different initial conditions on the variable x for these two cases. However, the condition $\theta(s, 0^+) = \theta(s, 0^-)$ assures continuity of the solution for all values of y .

For $y > 0$, the solution to the second order, linear differential equation has the general form

$$\tilde{\theta}(s, y) = A_1(s) \exp(y/\sqrt{sV_{\infty}/\alpha}) + B_1(s) \exp(-y/\sqrt{sV_{\infty}/\alpha}) \tag{B.10}$$

The condition for convergence as $y \rightarrow \infty$ requires that $A_1(s) = 0$, and the condition on $\tilde{\theta}(s, 0^+)$ requires $B_1(s) = 1/(2s)$. Therefore,

$$\tilde{\theta}(s, y) = \{1/(2s)\} \exp(-y/\sqrt{sV_{\infty}/\alpha}) \quad (y > 0) \tag{B.11}$$

For the case $y < 0$, the homogeneous solution is as given in (B.10), above, and a particular solution is $\tilde{\theta}_p(s, y) = 1/s$. The general solution for this case is then

$$\bar{\theta}(s,y) = 1/s + A_2(s)\exp(y/\sqrt{sV_\infty/\alpha}) + B_2(s)\exp(-y/\sqrt{sV_\infty/\alpha}) \quad (B.12)$$

Here, the condition for convergence as $y \rightarrow -\infty$ requires $B_2(s) = 0$. The condition on $\bar{\theta}(s,0^-)$ requires $A_2(s) = -1/(2s)$. Therefore,

$$\bar{\theta}(s,y) = 1/s - \{1/(2s)\}\exp(-|y|/\sqrt{sV_\infty/\alpha}) \quad (y < 0) \quad (B.13)$$

The inverse Laplace transforms of these functions are (ref 13):

$$\theta(x,y) = \frac{1}{2}\text{erfc}(y/\sqrt{4\alpha x/V_\infty}) \quad (y > 0) \quad (B.14)$$

$$\theta(x,y) = 1 - \frac{1}{2}\text{erfc}(|y|/\sqrt{4\alpha x/V_\infty}) \quad (y < 0) \quad (B.15)$$

where $\text{erfc}(x) = 1 - \text{erf}(x)$ and $\text{erf}(x)$ is given by

$$\text{erf}(x) = \frac{2}{\sqrt{\pi}} \int_0^x \exp(-\omega^2) d\omega \quad (B.16)$$

Determination of a Similarity Transformation

As noted earlier, it seems reasonable to expect isotherms to be plotted in the (x,y) plane as $y = kx^{(1/n)}$. In such a case it is possible to reduce the partial differential equation in x and y to an ordinary differential equation in terms of a similarity transformation $(x,y) \rightarrow$

η . To determine the appropriate functional relationship between η and (x,y) , the solution form is assumed to be

$$\eta = x^a y^b \left(\frac{\alpha}{V_\infty}\right)^c \quad (\text{B.17})$$

Using primes (') to denote differentiation with respect to η , we have

$$\begin{aligned} \frac{\partial \theta}{\partial x} &= \frac{\partial \theta}{\partial \eta} \frac{\partial \eta}{\partial x} = \theta' \frac{a\eta}{x} \\ \frac{\partial \theta}{\partial y} &= \frac{\partial \theta}{\partial \eta} \frac{\partial \eta}{\partial y} = \theta' \frac{b\eta}{y} \\ \frac{\partial^2 \theta}{\partial y^2} &= \frac{\partial \theta}{\partial \eta} \left(\theta' \frac{b\eta}{y} \right) \frac{\partial \eta}{\partial y} = \theta'' \frac{b^2 \eta^2}{y^2} - \theta' \frac{b^2}{y^2} \end{aligned} \quad (\text{B.18})$$

Substituting these expressions into equation B.5 yields

$$\frac{a}{x} \eta \theta' = \frac{(\alpha/V_\infty) b^2}{y^2} \eta^2 \theta'' + \eta \theta' \left(\frac{(\alpha/V_\infty) b^2}{y^2} - \frac{(\alpha/V_\infty) b}{y^2} \right) \quad (\text{B.19})$$

Multiplying this expression by $(\frac{x}{a})$ and simplifying yields

$$\eta \theta' = \left(\frac{b^2}{a}\right) \left(\frac{x(\alpha/V_\infty)}{y^2}\right) \eta^2 \theta'' + \left(\frac{b}{a}\right) \left(b \frac{x(\alpha/V_\infty)}{y^2} - \frac{x(\alpha/V_\infty)}{y^2}\right) \eta \theta' \quad (\text{B.20})$$

Inspection of equation B.20 suggests a similarity transformation of the form $\eta_1 = y^2/(\alpha x/V_\infty)$, in which case equation B.5 reduces to the ordinary differential equation

$$4\eta_1 \theta'' + (2 + \eta_1) \theta' = 0 \quad (\eta_1 = y^2/(\alpha x/V_\infty)) \quad (\text{B.21})$$

There is, however, a somewhat more convenient (and more conventional) choice for η . If b is chosen equal to unity, then the last term on the right hand side of equation B.19 is zero. The remaining term on the right hand side of the equation must have $(\alpha x/V_\infty)/y^2$ equal to η^p for self-similarity. Since b (the power of y) has already been chosen to be one, p must equal -2 .

An additional simplification occurs if η^2 is chosen to be $(ay)^2/(\alpha x/V_\infty)$ (i.e. $\eta = \pm(ay)/\sqrt{\alpha x/V_\infty}$, with the factor (a) absorbed into the non-dimensional variable). By the construction of η , a and c must be set equal to $-\frac{1}{2}$ so that $\eta = \pm y/\sqrt{4\alpha x/V_\infty}$. In this case, equation B.20 reduces to

$$\theta'' + 2\eta\theta' = 0 \quad (\eta = \pm y/\sqrt{4\alpha x/V_\infty}) \quad (B.22)$$

The solution to equation B.22 has the form $\theta = A + \text{Berf}(\eta)$. Application of the boundary conditions (B.7) again yields equations B.14 and B.15 as the required solution to the differential equation B.5.

Appendix C. Condensation and Icing

The equation of motion for a particle moving with respect to a fluid may be obtained by determining the forces which act on the particle and applying Newton's Second Law.

In general, three forces will act on such a particle: a buoyant force, equal in magnitude to the weight of the displaced fluid; a gravitational force, equal in magnitude to the weight of the particle; and a viscous drag force, which depends on the geometry of the particle under consideration and is directed to oppose the velocity of the particle relative to the fluid.

If the vector representing the acceleration due to gravity is assumed to be parallel to the y-axis, these forces can be modelled by:

$$\begin{aligned}\text{Buoyant force: } & (\rho_f \times \text{Vol} \times g)\hat{j} \\ \text{Gravitational force: } & -(\rho_p \times \text{Vol} \times g)\hat{j} \\ \text{Viscous Drag: } & -\{C_D(\frac{1}{2}\rho_f \bar{v}_r \cdot \bar{v}_r)A\}\hat{v}_r\end{aligned}\tag{C.1}$$

where the subscripts f and p refer to properties of the fluid and the particle, respectively; Vol is the volume of the particle and A is its frontal area; \bar{v}_r is the velocity of the particle relative to the fluid and \hat{v}_r is a unit vector aligned with \bar{v}_r ; and C_D is the non-dimensional coefficient of drag based on frontal area.

The value of C_D is dependent on the geometry of the particle and on the Reynolds number of the particle with respect to the fluid.

If the particle can be approximated as a sphere then C_D as a function of Re can be determined from the plot found on page 17 of ref 1. For the purpose of integrating the equation of motion for the particle it is most convenient to establish an empirical functional relationship between C_D and Re .

Stoke's approximation gives $C_D = 24/Re$ for very low Reynolds numbers, and C_D is approximately constant for the range $2000 < Re < 200,000$ ($C_D = 0.405$). In the intermediate range, $0.25 < Re < 2000$, the data suggests a polynomial relationship between $\log_{10} C_D$ and $\log_{10} Re$.

Therefore, relationships of the form

$$\begin{aligned}\zeta &= A\xi^4 + B\xi^3 + C\xi^2 + D\xi + E \\ \zeta &= F\xi^2 + G\xi + H \\ \zeta &= \log_{10} C_D \\ \xi &= \log_{10} Re\end{aligned}\tag{C.2}$$

are assumed, and a least-squares curve can be fitted to the data presented in ref 1. The results of these curve fits are:

$$\zeta = 0.00311\xi^4 - 0.140\xi^3 + 0.115\xi^2 - 0.888\xi + 1.42 \tag{C.3}$$

$$\zeta = 0.102\xi^2 - 0.894\xi + 1.42 \tag{C.4}$$

Table C.1 compares the values of C_D from ref 1 with those obtained using the quadratic and quartic polynomial approximations given above. In both cases, agreement between the accepted value and the approximation is very good (within three per cent in most cases).

For the situation under consideration here, Re is to be evaluated using the magnitude of \bar{v}_r . With this relationship between \bar{v}_r and C_D , the equation of motion for a sphere can be numerically integrated to obtain $\bar{v}_r(t)$ and again to determine the position vector, $\bar{r}(t)$.

Let the velocity of the particle be denoted by $\bar{v}(t) = u(t)\hat{i} + v(t)\hat{j}$ (note that $\bar{v}(t)$ is not the relative velocity between the particle and the fluid). If the spherical particle is assumed to have been formed instantaneously at time $t = 0$, then $\bar{v}(0) = \bar{V}_\infty$, where \bar{V}_∞ is the vector representing the fluid velocity. For the case where the free stream velocity is perpendicular to the gravitational acceleration vector, $\bar{V}_\infty = V_\infty\hat{i}$.

A qualitative argument establishes the fact that $u(t) \equiv V_\infty$ under these conditions. Since the drag force depends on the relative velocity between the particle and the fluid, there can be no viscous drag on the particle at time $t = 0$. The gravitational and buoyant forces do not affect the x-component of velocity, so $u(\Delta t)$ must equal

V_∞ . At time $t = \Delta t$, therefore, \bar{v}_r must be perpendicular to the free stream velocity with no component in the x-direction. This argument can be extended to any time

Table C.1. Comparison of Equations C.3 and C.4 with Measured Data

Re	C_D (ref 1)	Quartic C_D	Quartic Approx. Error	Quadratic C_D	Quadratic Approx. Error
0.4	62	62	0	62	0
0.6	42	42	0	42	0
0.8	33	32	- 3.0%	32	- 3.0%
1.0	26.5	26.3	- 0.8%	26.3	- 0.8%
2	14.5	14.5	0	14.4	- 0.7%
4	8.4	8.4	0	8.3	- 1.2%
6	6.1	6.2	+ 1.6%	6.1	0
8	5.1	5.0	- 2.0%	5.0	- 2.0%
10	4.35	4.33	- 0.4%	4.25	- 2.3%
20	2.75	2.74	- 0.4%	2.69	- 2.2%
40	1.8	1.8	0	1.8	0
60	1.45	1.44	- 0.7%	1.42	- 2.1%
80	1.2	1.2	0	1.2	0
100	1.13	1.10	- 2.6%	1.10	- 2.6%
200	0.81	0.80	- 1.2%	0.80	- 1.2%
400	0.61	0.61	0	0.61	0
600	0.53	0.53	0	0.53	0
800	0.49	0.47	0	0.48	- 2.0%
1000	0.46	0.46	0	0.45	- 2.2%
2000	0.41	0.40	- 2.4%	0.38	- 7.3%

t to show that, for $\bar{V}_\infty = \bar{V}_\infty \hat{i}$, there can be no x-component to the vector \bar{v}_r .

Furthermore, this yields the result that $\hat{v}_r = \pm \hat{j}$, and since the spherical particle is expected to fall under the influence of gravity, $\hat{v}_r = -\hat{j}$.

Therefore, for the case under consideration the equations of motion are given by

$$\begin{aligned} u(t) &\equiv V \\ \rho_p \times \text{Vol} \times \dot{v} &= (\rho_f - \rho_p) \times \text{Vol} \times g \\ &\quad + C_D \left(\frac{1}{2} \rho_f v^2 A \right) \\ v(0) &= 0 \end{aligned} \tag{C.5}$$

The volume of a sphere is given by $\frac{4}{3}\pi r^3$, and its frontal area is πr^2 . Using these relationships in the equation above and dividing both sides by $\rho_p \times \text{Vol}$ yields the following result:

$$\begin{aligned} u(t) &\equiv V \\ \dot{v} &= (\hat{\rho}-1)g + C_D(3/8r)\hat{\rho}v^2 \\ v(0) &= 0 \end{aligned} \tag{C.6}$$

where $\hat{\rho}$ is defined by $\hat{\rho} = \rho_f/\rho_s$. It is also convenient to define the parameter g^* to be $g^* = (\hat{\rho}-1)g$. A good approximation to this value is $g^* = 32.1 \text{ ft/sec}^2$.

When the acceleration due to effective gravitational force (g^*) is balanced by the viscous drag force, the

spherical particle will fall at a constant velocity for all time from that point on. This possibility must be accounted for before attempting a numerical solution to equation C.6. For this purpose, the condition $\dot{v} = 0$ if $C_D(3/8r)\hat{\rho}v^2 > g^*$ is added to equation C.6.

Several types of numerical schemes were used to integrate equation C.6. When these schemes were compared it was determined that a simple forward differencing technique gave sufficient accuracy in its results. The forward difference equations employed in this algorithm are:

$$\begin{aligned} v(t+\Delta t) &= v(t) + \Delta t(C_D(3/8r)\hat{\rho}v^2 - 32.1), \text{ if} \\ &\quad C_D(3/8r)\hat{\rho}v^2 < 32.1 \\ v(t+\Delta t) &= 0, \text{ otherwise} \\ v(0) &= 0 \end{aligned} \tag{C.7}$$

For the purposes of this study, the fluid properties were taken to be those of nitrogen at -280 F and 1 atm pressure and the value of ρ_p was chosen to be the density of water at 32 F.

The numerical integration was performed on a Hewlett-Packard model 9845 desktop computer using a program written in BASIC. The results of the numerical integration for some values of r and Δt are presented in the tables which follow.

Table C.2.
Results of the Numerical Integration of Equation C.7.
 $\Delta t = 0.1$ sec

t (sec)	Distance Travelled (ft)		
	2r=0.05 ft	2r=0.01 ft	2r=0.005 ft
0.1	0.16	0.16	0.16
0.2	0.64	0.64	0.64
0.3	1.4	1.4	1.4
0.4	2.5	2.4	2.3
0.5	3.9	3.7	3.4
0.6	5.6	5.1	4.5
0.7	7.6	6.6	5.7
0.8	9.7	8.2	6.9
0.9	12	9.8	8.1
1.0	15	11	9.4

Table C.3.
Results of the Numerical Integration of Equation C.7.
 $\Delta t = 0.01$ sec

t (sec)	Distance Travelled (ft)	
	2r=0.05 ft	2r=0.01 ft
0.01	0.0016	0.0016
0.02	0.0064	0.0064
0.03	0.014	0.014
0.04	0.026	0.026
0.05	0.040	0.040
0.06	0.058	0.058
0.07	0.079	0.078
0.08	0.10	0.10
0.09	0.13	0.13
0.10	0.16	0.16

Appendix D. Property Values and Sample Calculations

In order to determine the values for the various parameters which have been shown to be important in this Reynolds number simulation technique (e.g., Re , L), it is necessary to obtain various property values as functions of pressure and temperature. In many cases, these values can be read from tables (see, for example refs 14 and 15). For convenience, expressions which can be used to evaluate many of these properties are summarized below.

Density

From the ideal gas law, the value for density can be determined from $\rho = \frac{p}{RT}$, where R is the gas constant for the particular gas.

The value of R is determined from $R = \tilde{R}/M$, where \tilde{R} is the universal gas constant (1545.43 (ft-lb_f/R-lb_m mole)) and M is the molecular weight of the gas. For air, $R \approx 1716$ ft²/R-sec² and for nitrogen, $R \approx 1775$ ft²/R-sec².

Viscosity

The coefficient of viscosity, μ , is not strongly dependent on pressure. An empirical relationship between

μ and T is given by Sutherland's law to within $\pm 2\%$ when T is within prescribed limits. The relationship is

$$\frac{\mu}{\mu_0} = \left(\frac{T}{T_0}\right)^{3/2} \frac{T_0 + S}{T + S} \quad (D.1)$$

For nitrogen: $\mu_0 = 3.473 \times 10^{-7}$ slug/ft-sec, $T_0 = 491.6$ R, $S = 192$ R, and $180 \text{ R} < T < 2700 \text{ R}$.

For air: $\mu_0 = 3.584 \times 10^{-7}$ slug/ft-sec, $T_0 = 491.6$ R, $S = 199$ R, and $300 \text{ R} < T < 3420 \text{ R}$.

The value for the kinematic viscosity, ν , can be determined from the relationship $\nu = \mu/\rho$.

Thermal Conductivity

A Sutherland's law relationship also exists for the coefficient of thermal conductivity, k .

$$\frac{k}{k_0} = \left(\frac{T}{T_0}\right)^{3/2} \frac{T_0 + S}{T + S} \quad (D.2)$$

For nitrogen: $k_0 = 0.0140$ B/h-ft-R, $T_0 = 491.6$ R, $S = 300$ R, and $260 \text{ R} < T < 2160 \text{ R}$.

For air: $k_0 = 0.01395$ B/h-ft-R, $T_0 = 491.6$ R, $S = 350$ R, and $300 \text{ R} < T < 1800 \text{ R}$.

The value for thermal diffusivity, α , can be derived from $\alpha = k/\rho c_p$.

Sample Calculation

In order to illustrate the use of the techniques outlined in the paper to simulate high Reynolds number flow, a sample calculation is carried out below:

It is desired to simulate $Re \approx 1 \times 10^7$ on a flat plate two feet long and one foot wide. The tunnel total temperature is approximately 540 R, and total pressure (for the tunnel air) is about 1 atm ($2117 \text{ lb}_f/\text{ft}^2$).

Liquid nitrogen is used as the cool fluid, so its properties are evaluated at $T_c = 180 \text{ R}$. From ref 14,

$$\mu_c = 4.611 \times 10^{-6} \text{ lb}_m/\text{sec-ft} = 1.432 \times 10^{-7} \text{ slug/sec-ft}$$

$$k_c = 5.460 \times 10^{-8} \text{ B/h-ft-R}$$

At a pressure of 1 atm, the density of nitrogen is $0.2173 \text{ lb}_m/\text{ft}^3$; this value can be used to determine the required V_∞ .

$$\begin{aligned} Re &= \rho_c V_\infty \ell / \mu_c = 1 \times 10^7, \text{ so} \\ V_\infty &= (1 \times 10^7) / (\rho_c \ell / \mu_c) \end{aligned} \tag{D.3}$$

The quantity $\rho_c \ell / \mu_c$ is approximately 9.42×10^4 , so the required velocity is $V \approx 106 \text{ ft/sec}$.

Chapter V outlines the procedure for determining p_c from V_∞ , T_t , and p_t .

The density of the tunnel air, ρ_s , is assumed equal to $2.3 \times 10^{-3} \text{ slugs/ft}^3$ at $T_s = 540 \text{ R}$.

$$\begin{aligned}
 q &= \frac{1}{2} \rho_s V_\infty^2 = \frac{1}{2} (2.3 \times 10^{-3}) (106)^2 = 12.92 \text{ lb}_f/\text{ft} \\
 p_s &= p_t - q = 2117 - 12.92 \approx 2104 \text{ lb}_f/\text{ft}^2 \\
 p_s/p_t &\approx 0.994
 \end{aligned}
 \tag{D.4}$$

For air at low temperatures, $\gamma = 1.4$, and the ratio $(\gamma-1)/\gamma \approx 0.286$. The isentropic relations give

$$T_s = 0.998 T_t \approx T_t = 540 \text{ R} \tag{D.5}$$

and $\gamma'(T_s = 540) \approx \gamma = 1.4$, so $T_s \approx 540 \text{ R}$.

The value of ρ_s' is found from the ideal gas law.

$$\begin{aligned}
 \rho_s' &= p_s / R_s T_s = 2104 / (1716 \times 540) = 2.27 \times 10^{-3} \text{ slugs/ft}^3 \\
 &\approx \rho_s
 \end{aligned}
 \tag{D.6}$$

Since $\rho_s \approx \rho_s'$, p_s can be taken as $2104 \text{ lb}_f/\text{ft}^2$, and therefore $p_c = p_s = 2104 \text{ lb}_f/\text{ft}^2$.

It is now possible to determine the values v_c and α_c .

$$\begin{aligned}
 \rho_c &= p_c / R_c T_c = 2104 / (1775 \times 180) = 6.58 \times 10^{-3} \text{ slugs/ft}^3 \\
 v_c &= \mu_c / \rho_c = 1.432 \times 10^{-7} / 6.58 \times 10^{-3} = 2.176 \times 10^{-5} \text{ ft}^2/\text{sec} \\
 \alpha_c &= k_c / \rho_c c_{p_c} = 5.46 \times 10^{-3} / (6.58 \times 10^{-3} \times 0.255) \\
 &= 3.254 \text{ lb}_m\text{-ft}^2/\text{slug-hr} = 0.101 \text{ ft}^2/\text{hr} \\
 &= 2.807 \times 10^{-5} \text{ ft}^2/\text{sec}
 \end{aligned}
 \tag{D.7}$$

where the value of c_{p_c} has been taken as $0.255 \text{ B/lb}_m\text{-R}$.

With these values for α_c and v_c , it is possible to determine the value of the parameter L . Since the boundary layer is expected to be turbulent for $Re = 1 \times 10^7$, the value to be calculated is $L_t = 3.3\sqrt{\alpha_c/V_\infty} + 0.37\sqrt[5]{v_c/V_\infty}\ell^{3/10}$.

$$\begin{aligned}\sqrt{\alpha_c/V_\infty} &= \sqrt{2.807 \times 10^{-5}/106} = 5.146 \times 10^{-4} \text{ ft}^{1/2} \\ \sqrt[5]{v_c/V_\infty} &= \sqrt[5]{2.176 \times 10^{-5}/106} = 4.597 \times 10^{-2} \text{ ft}^{1/5} \\ \ell^{3/10} &= 2^{3/10} = 1.23 \text{ ft}^{3/10}\end{aligned}\tag{D.8}$$

This gives $L_t = 2.262 \times 10^{-2} \text{ ft}^{1/2}$. The constraint on h requires $h > L_t\sqrt{x}$, and $L_t\sqrt{x} \approx 0.032 \text{ ft}$, so

$$h > 0.032 \text{ ft}\tag{D.8}$$

To determine the required mass rate of flow, the applicable constraint is $\dot{m}/w > \rho_c V_\infty L_t\sqrt{x}$, so

$$\dot{m}/w > 6.58 \times 10^{-3} \times 106 \times 0.032 = 2.23 \times 10^{-2} \text{ slugs/ft-sec}\tag{D.9}$$

For the plate under consideration, $w = 1 \text{ ft}$, so

$$\dot{m} > 2.23 \times 10^{-2} \text{ slugs/sec} = 0.719 \text{ lb}_m/\text{sec}\tag{D.10}$$

If condensation or icing is expected to be a problem, the value ℓ/V_∞ should be calculated and then used to see if condensation will effect the boundary layer.

For this exercise, $\ell/V_\infty \approx 0.02 \text{ sec}$. A spherical par-

ticle with a diameter of 0.01 ft (about $\frac{1}{8}$ in) will fall approximately 0.006 ft (0.07 in) in this time. For the case under consideration, $h \gg 0.006$ ft, so condensation and icing are not expected to effect the Reynolds simulation.

The value for the Reynolds number can be determined from the flow properties which have been established above.

$$Re_c = V_\infty \ell / \nu_c = (106)(2) / 2.176 \times 10^{-5} = 9.74 \times 10^6 \quad (D.11)$$

This is very close to the desired value of $Re = 1 \times 10^7$.

It is instructive to calculate the value of Re_s , the Reynolds number based on properties of the tunnel air. It has already been established that $\rho_s = 2.27 \times 10^{-3}$ slugs/ft³, and μ_s is found to be 3.854×10^{-7} slugs/sec-ft. Therefore, $\nu_s = 1.698 \times 10^{-4}$ ft²/sec, and

$$Re_s = V_\infty \ell / \nu_s = (106)(2) / 1.698 \times 10^{-4} = 1.25 \times 10^6 \quad (D.12)$$

From this, the ratio Re_c / Re_s can be found to be 7.8. The cooling technique described in this paper has therefore resulted in an increase in effective Reynolds number of nearly an order of magnitude.

Appendix E. The Parameter L

The parameter L which appears in the statement of constraints developed in Chapter V contains all of the information regarding the temperature dependency of those constraints.

This temperature dependency can be made explicit by applying the Sutherland's law equations presented in Appendix D along with the ideal gas law.

From the ideal gas law,

$$\frac{\rho}{\rho_0} = \left(\frac{p}{T}\right) \left(\frac{T_0}{p_0}\right) = \left(\frac{T_0}{T}\right) \left(\frac{p}{p_0}\right) \quad (\text{E.1})$$

where T_0 is taken as 491.6 R, $p_0 = 1$ atm, and $\rho_0 = p_0/RT_0$.

If ν_0 is defined to be μ_0/ρ_0 , then Sutherland's law gives

$$\frac{\nu}{\nu_0} = \left\{ \left(\frac{T}{T_0}\right)^{5/2} \frac{T_0 + S}{T + S} \right\} \left(\frac{p_0}{p}\right) \quad (\text{E.2})$$

A similar expression can be developed for the thermal diffusivity, α . If c_p is assumed constant, and for $\alpha_0 = k_0/\rho_0 c_p$, the result is

$$\frac{\alpha}{\alpha_0} = \left\{ \left(\frac{T}{T_0}\right)^{5/2} \frac{T_0 + S^*}{T + S^*} \right\} \left(\frac{p_0}{p}\right) \quad (\text{E.3})$$

The values for S , S^* , and T_0 are given in Appendix D.

In the case where the tunnel pressure, p_g , is nearly the same as atmospheric pressure, the quantity p_0/p is nearly unity. With this assumption, and from the definition of L , the temperature dependence of L is expressed as

$$L_\ell = \left(\frac{T}{T_0}\right)^{5/4} \left\{ \sqrt{\alpha_0/V_\infty} \left(\frac{T_0+S^*}{T+S^*}\right)^{1/2} + \sqrt{v_0/V_\infty} \left(\frac{T_0+S}{T+S}\right)^{1/2} \right\} \quad (E.4)$$

$$L_x = \left(\frac{T}{T_0}\right)^{5/4} \left\{ \sqrt{\alpha_0/V_\infty} \left(\frac{T_0+S^*}{T+S^*}\right)^{1/2} \right\} + \left(\frac{T}{T_0}\right)^{1/2} \left\{ \sqrt{v_0/V_\infty} \left(\frac{T_0+S}{T+S}\right)^{1/2} \right\} \ell^{3/10} \quad (E.5)$$

From equations E.4 and E.5 it is apparent that L is an increasing function of temperature, as well as an increasing function of free stream tunnel velocity. These characteristics are illustrated in the figures that follow.

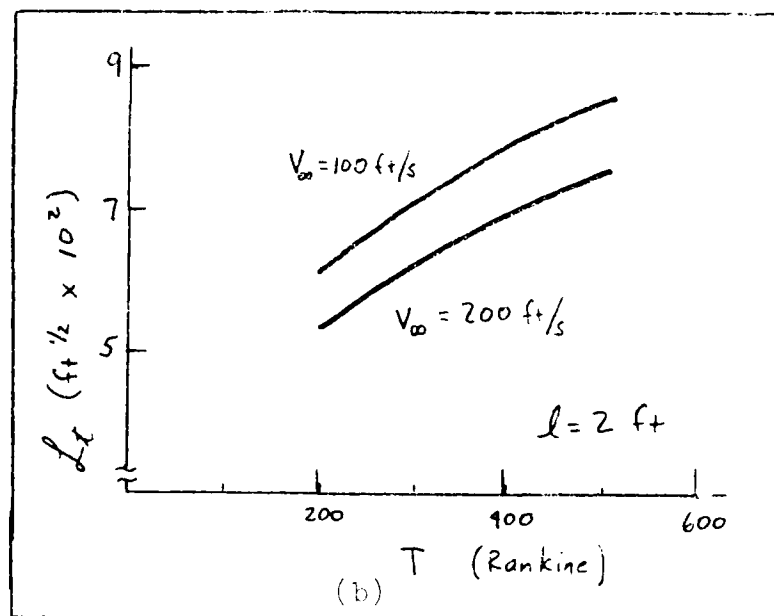
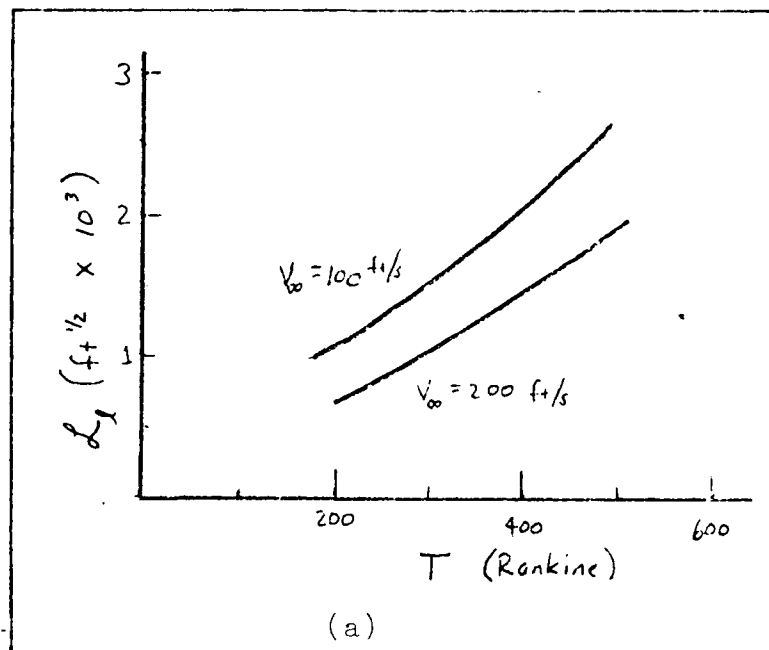


Figure E.1. Functional Dependence of L on Temperature for
 (a) Laminar Flow and (b) Turbulent Flow with $l = 2 \text{ ft}$.

AD-A141 062

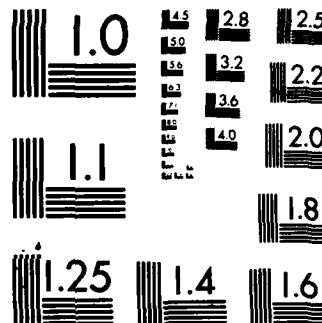
AN ANALYTICAL STUDY OF A LOCALLY COOLED HIGH REYNOLDS
NUMBER SIMULATION TECHNIQUE(U) AIR FORCE INST OF TECH
WRIGHT-PATTERSON AFB OH SCHOOL OF ENGI... M S BORKOWSKI
MAR 84 AFIT/GA/AA/84M-1 F/G 20/4

2/2

UNCLASSIFIED

NL





MICROCOPY RESOLUTION TEST CHART
NATIONAL BUREAU OF STANDARDS-1963-A

VITA

Mark S. Borkowski was born on September 16, 1958 in Killeen, Texas to Julian T. and Marie E. Borkowski. He graduated from McQuaid Jesuit High School (Rochester, NY) in 1976, and attended the State University of New York at Albany where he majored in Mathematics and received a Bachelor of Science degree in May 1980. He joined the United States Air Force and began Officer Training School in April 1981. He was named the First Honor Graduate of his OTS class and was commissioned in July 1981. Lt. Borkowski was assigned to the Air Force Institute of Technology as a student in the Undergraduate Aeronautical Engineering Program. He graduated from AFIT as a Distinguished Graduate and received a Bachelor of Science degree in Aeronautical Engineering in March 1983. He was then assigned to continue studies at AFIT as a student in the Graduate Astronautical Engineering Program.

Permanent address: 95 Cape Cod Way
Rochester, NY
14623

END

FILMED

6-84

DTIC